Article

SOURCE DATA | TRANSPARENT PROCESS

THE EMBO JOURNAL

Dopamine signaling promotes the xenobiotic stress response and protein homeostasis

Kishore K Joshi, Tarmie L Matlack & Christopher Rongo*

Abstract

Multicellular organisms encounter environmental conditions that adversely affect protein homeostasis (proteostasis), including extreme temperatures, toxins, and pathogens. It is unclear how they use sensory signaling to detect adverse conditions and then activate stress response pathways so as to offset potential damage. Here, we show that dopaminergic mechanosensory neurons in *C. elegans* release the neurohormone dopamine to promote proteostasis in epithelia. Signaling through the DA receptor DOP-1 activates the expression of xenobiotic stress response genes involved in pathogenic resistance and toxin removal, and these genes are required for the removal of unstable proteins in epithelia. Exposure to a bacterial pathogen (*Pseudomonas aeruginosa*) results in elevated removal of unstable proteins in epithelia, and this enhancement requires DA signaling. In the absence of DA signaling, nematodes show increased sensitivity to pathogenic bacteria and heat-shock stress. Our results suggest that dopaminergic sensory neurons, in addition to slowing down locomotion upon sensing a potential bacterial feeding source, also signal to frontline epithelia to activate the xenobiotic stress response so as to maintain proteostasis and prepare for possible infection.

Keywords xenobiotic stress; ubiquitin; proteostasis; dopamine; *C. elegans*
Subject Categories Microbiology, Virology & Host Pathogen Interaction; Neuroscience; Protein Biosynthesis & Quality Control
DOI 10.15252/embj.201592524 | Received 10 July 2015 | Revised 14 April 2016 | Accepted 3 May 2016 | Published online 3 June 2016
The EMBO Journal (2016) 35: 1885–1901

See also: **YL Chew & WR Schafer** (September 2016)

Introduction

Multicellular organisms develop and interact with an ever-changing environment, which can present conditions that impair development as well as physiology at the cellular and organismal level. Extreme temperatures, toxins, and pathogens present major physiological challenges, including challenges to the cell for maintaining protein homeostasis (proteostasis)—the natural folding and function of the cellular proteome (Shore & Ruvkun, 2013; Warnatsch *et al*, 2013; Vilchez *et al*, 2014; Treweek *et al*, 2015). The failure to maintain proteostasis in the face of such environmental challenges results in physiological decline, as oxidized and unfolded proteins threaten cellular physiology.

Most organisms have evolved multiple stress response pathways that act at the cellular level to help maintain proteostasis. For example, elevated temperatures can result in the unfolding and misfolding of proteins, and cells respond by elevating the transcription of heat-shock proteins (HSPs), some of which act as chaperones to help proteins fold properly even under higher temperature (Akerfelt *et al*, 2010; Murshid *et al*, 2013). Oxidative and xenobiotic stress can also damage proteins, DNA, and other macromolecules, and the oxidative stress response pathway, mediated by the transcription factor Nrf2, acts to offset the resulting reactive oxygen species (ROS) and protect macromolecules from oxidative and xenobiotic damage (Nguyen *et al*, 2009; Bock, 2014). Damaged and unfolded proteins are removed by the ubiquitin proteasome system (UPS), which covalently attaches chains of the small protein ubiquitin to lysine side chains of each protein substrate (Ciechanover & Stanhill, 2014). Such poly-ubiquitinated substrates are removed by proteolysis via the 26S proteasome. Alternatively, poly-ubiquitinated, aggregation-prone proteins that are resistant to degradation by the proteasome can be isolated within cells and degraded in autophagosomes after recognition by the autophagy pathway (Kirkin *et al*, 2009; Ryno *et al*, 2013; Ciechanover & Kwon, 2015; Cortes & La Spada, 2015; Lim & Yue, 2015). Membrane proteins can also be refolded and/or removed in the ER by the unfolded protein response (UPR) pathway (Ryno *et al*, 2013). Whereas these different stress response pathways are effective at the level of individual cells, it remains unclear how multicellular organisms coordinate these pathways over multiple differentiated tissues.

Changes in proteostasis in one tissue can alter proteostasis in other tissues (Van Oosten-Hawle & Morimoto, 2014). In *C. elegans*, the thermosensory neuron AFD senses acute heat stress and releases the neurotransmitter serotonin, which is then able to activate the expression of HSPs in distal tissues in response (Prahlad *et al*, 2008; Tatum *et al*, 2015). Similarly, the sensory neurons ASH and ASI can modulate the UPR in distal tissues like the intestine in a process that requires the octopamine receptor OCTR-1 (although octopamine is unlikely to be the neuron-to-intestine signal itself) (Sun *et al*, 2011, 2012). Although neuronal signaling likely provides a primary mechanism for regulating stress response across tissues, direct signaling

Department of Genetics, The Waksman Institute, Rutgers The State University of New Jersey, Piscataway, NJ, USA
*Corresponding author. Tel: +1 848 445 0955; Fax: +1 732 445 5735; E-mail: rongo@waksman.rutgers.edu

between non-neuronal tissues has also been shown to regulate the heat-shock response and longevity in a non-autonomous fashion (Van Oosten-Hawle *et al*, 2013; Van Oosten-Hawle & Morimoto, 2014). Clearly, non-autonomous signaling between tissues conveys information about changes in proteostasis internal to the organism. Yet it remains unclear how animals use sensory signaling to detect external (environmental) cues indicative of adversity and activate stress response pathways so as to offset potential damage (Aballay, 2013; Van Oosten-Hawle & Morimoto, 2014; Volovik *et al*, 2014; Mardones *et al*, 2015).

Another proteostasis protection mechanism that can be modulated non-autonomously is the ubiquitin proteasome system (UPS). For example, germ line ablation activates the expression of the proteasome subunit RPN-6 in *C. elegans* via regulation by the DAF-16 (FOXO) transcription factor (Vilchez *et al*, 2012). In addition, EGF signaling can augment UPS activity in epithelial cells as *C. elegans* enter their period of peak fecundity (Liu *et al*, 2011). Reduced UPS activity, particularly as an organism ages, leads to a decline in proteostasis. This is a bidirectional relationship, as a decline in proteostasis (e.g., due to the impairment of chaperones and other protein quality control mechanisms) leads to changes in UPS activity. Thus, the exact relationship between non-autonomous sensory signaling, UPS activity, and other protein quality control systems remains uncertain.

To identify novel regulators of UPS activity and proteostasis, we used a transgenic approach in *C. elegans* by monitoring UPS activity using the ubiquitin fusion degradation (UFD) substrate Ub^{G76V}-GFP, an unstable protein that is comprised of a non-cleavable ubiquitin placed amino-terminal to GFP (Liu *et al*, 2011; Segref *et al*, 2011). Ub^{G76V}-GFP mimics a mono-ubiquitinated protein, and additional ubiquitins are attached by the UFD complex to K48 residues located on the N-terminal ubiquitin, eventually resulting in a poly-ubiquitinated substrate that is degraded by the 26S proteasome (Butt *et al*, 1988; Johnson *et al*, 1995; Dantuma *et al*, 2000). Ub^{G76V}-GFP degradation was previously monitored in *C. elegans* intestinal or hypodermal epithelia when this UFD substrate was expressed from either the *sur-5* or *col-19* promoter, respectively (Liu *et al*, 2011; Segref *et al*, 2011). Using this reporter, here we have screened for genes that play a role is regulating Ub^{G76V}-GFP degradation in the epithelia. We found that the neurotransmitter dopamine (DA), which is made by mechanosensory neurons in *C. elegans* and used to transmit information about surrounding environmental viscosity to the motoneurons so as to modulate feeding behavior (Sawin *et al*, 2000; Chase *et al*, 2004; Kindt *et al*, 2007; Suo & Ishiura, 2013), also functions to modulate Ub^{G76V}-GFP turnover in epithelia. In the absence of DA signaling or mechanosensation of the external environment, intestinal and hypodermal epithelia show increased stability of the otherwise unstable Ub^{G76V}-GFP reporter protein. The regulation of Ub^{G76V}-GFP degradation by DA signaling requires the cAMP response element binding protein transcription factor (CREB) and the ELT-3 GATA transcription factor, and we find by expression profile analysis that DA signaling promotes the expression of the xenobiotic stress response genes. These genes, in turn, are required for DA to modulate Ub^{G76V}-GFP degradation. Failure to signal through DA and its receptors results in animals with altered proteostasis, impaired survival at high temperature, increased sensitivity to infection by pathogenic bacteria, and increased sensitivity of unstable proteins to reactive oxygen species (ROS) exposure. Our results suggest that dopaminergic sensory neurons, in addition to slowing down locomotion upon sensing a potential bacterial feeding source, also signal to epithelial tissues to modulate proteostasis and prepare for infection by a potential bacterial pathogen.

Results

Dopaminergic signaling modulates protein turnover

In order to examine changes in UPS activity, we employed previously described transgenic strains that express an Ub^{G76V}-GFP reporter, allowing us to monitor Ub^{G76V}-GFP degradation in *C. elegans* intestinal or hypodermal epithelia when the reporter was expressed from either the *sur-5* or *col-19* promoter, respectively (Liu *et al*, 2011; Segref *et al*, 2011). Ub^{G76V}-GFP levels inversely reflect the ability of the UPS to remove damaged and unstable proteins. Moreover, Ub^{G76V}-GFP levels can be compared to a relatively stable control protein (either mCherry or mRFP) expressed from the same promoter to rule out differences due to transgene expression (Fig 1A). In hypodermis, the expression of Ub^{G76V}-GFP and mRFP from the *col-19* promoter beginning at the L4 stage of development results in the rapid accumulation of both proteins within 24 h (L4 + 24 h; Fig 1B). However, Ub^{G76V}-GFP is rapidly degraded upon entering the period of peak fecundity (L4 + 48 h and onward, Fig 1B–D). We also examined Ub^{G76V}-GFP in transgenic animals expressing Ub^{G76V}-GFP from the *sur-5* promoter, focusing on intestinal expression of the reporter from this broadly expressed promoter. We found a similar turnover of the protein in intestine by L4 + 48 h as that observed in hypodermis (Fig 1E and F). Ub^{G76V}-GFP degradation is mediated in part by poly-ubiquitination by the UFD E3/E4 ligase complex and proteolysis by the 26S proteasome (Liu *et al*, 2011; Segref *et al*, 2011). We reconfirmed this finding by performing RNAi of subunits from these complexes, which resulted in increased peak accumulation of Ub^{G76V}-GFP at L4 + 24 h, as well as a slower rate of Ub^{G76V}-GFP turnover and a plateaued steady state level of Ub^{G76V}-GFP at later time points (Fig 1B). The levels of the unstable Ub^{G76V}-GFP protein therefore provide an index of UPS activity and proteostasis.

We used the Ub^{G76V}-GFP reporter in the hypodermis to perform an RNAi screen for regulators of UPS activity, screening an RNAi library enriched for signal transduction molecules, synaptic proteins cytoskeletal regulators, and membrane trafficking molecules (Sieburth *et al*, 2005). From 2,072 screened clones, we identified 31 RNAi candidates with altered Ub^{G76V}-GFP/mRFP ratios at the L4 + 48 h time point. Particularly striking from this screen was the stabilization of Ub^{G76V}-GFP in animals knocked down for a receptor for the neurotransmitter dopamine (DA). We hypothesized that dopamine signaling might regulate proteostasis and investigated this hypothesis by examining Ub^{G76V}-GFP in true mutants for genes involved in DA signaling. For example, loss-of-function mutations in the DA receptor *dop-1* resulted in elevated Ub^{G76V}-GFP levels in both the intestine and the hypodermis (Fig 1G–K). Animals deficient in DA synthesis itself showed a similar phenotype. CAT-2 encodes tyrosine hydroxylase, which is essential for DA synthesis (Lints & Emmons, 1999), and we found that loss-of-function mutants for *cat-2* contained elevated ratios of Ub^{G76V}-GFP to mRFP in the hypodermis at L4 + 48 h (Fig 1K and L). We found that three independently isolated loss-of-function alleles in the receptor *dop-1*, a D1-like DA receptor (DAR), resulted in elevated Ub^{G76V}-GFP in both

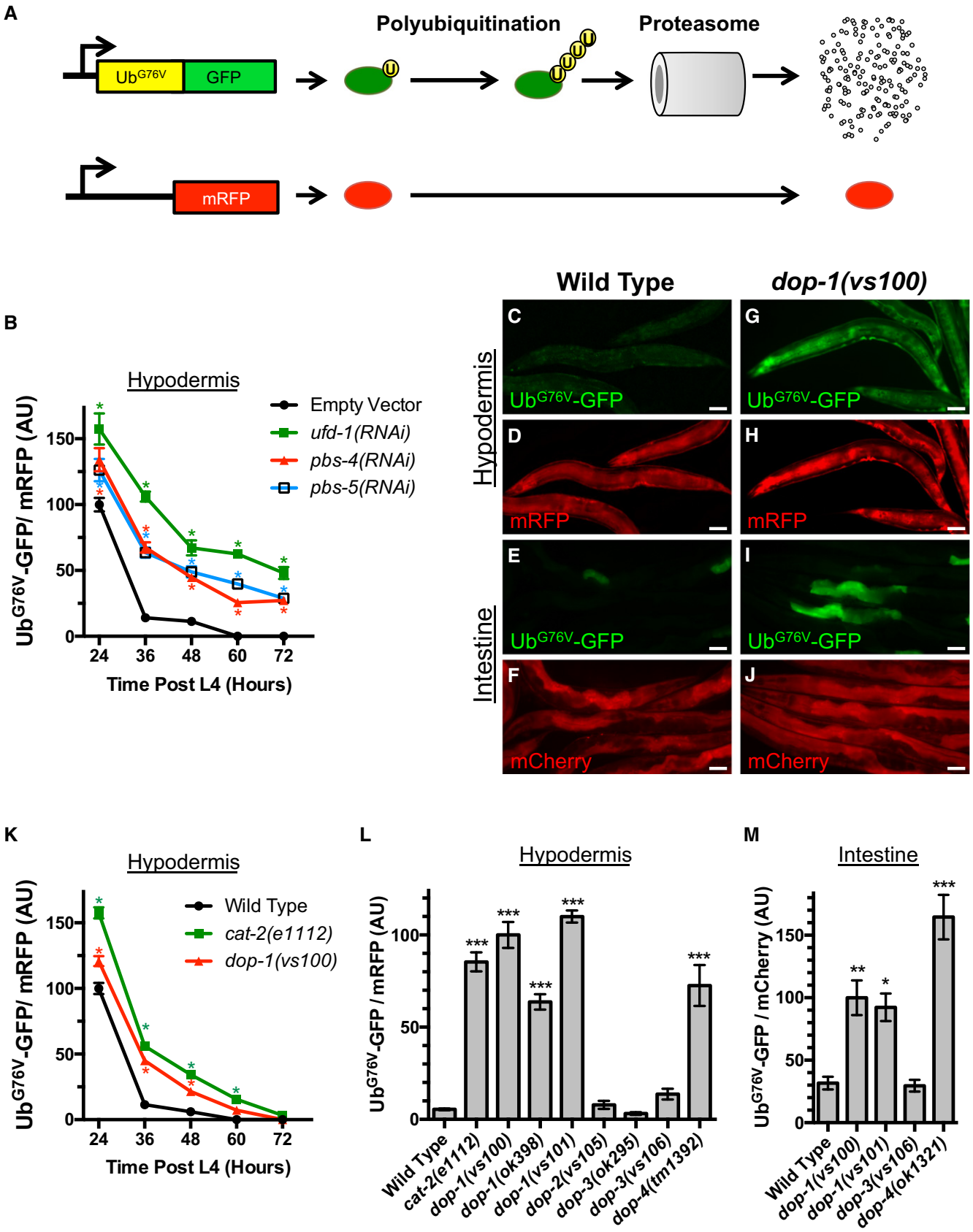
A
Polyubiquitination
Proteasome
UbG76V
GFP
mRFP
B
Hypodermis
Empty Vector
ufd-1(RNAi)
pbs-4(RNAi)
pbs-5(RNAi)
UbG76V-GFP/ mRFP (AU)
Time Post L4 (Hours)
Wild Type
dop-1(vs100)
Hypodermis
Intestine
C
G
D
H
E
I
F
J
UbG76V-GFP
mRFP
mCherry
K
Hypodermis
Wild Type
cat-2(e1112)
dop-1(vs100)
UbG76V-GFP/ mRFP (AU)
Time Post L4 (Hours)
L
Hypodermis
UbG76V-GFP / mRFP (AU)
Wild Type
cat-2(e1112)
dop-1(vs100)
dop-1(ok398)
dop-1(vs101)
dop-2(vs105)
dop-3(ok295)
dop-3(vs106)
dop-4(tm1392)
M
Intestine
UbG76V-GFP / mCherry (AU)
Wild Type
dop-1(vs100)
dop-1(vs101)
dop-3(vs106)
dop-4(ok1321)

Figure 1.

Figure 1. Dopaminergic signaling modulates protein turnover.

A Schematic representation of the Ub^{G76V}-GFP chimeric reporter and its associated internal control (mRFP or mCherry, in red). The amino acid sequences for ubiquitin are in yellow, whereas the sequences for GFP are in green. The Ub^{G76V}-GFP chimera, which contains a mutation in the terminal residue of ubiquitin, cannot be cleaved. The resulting protein is a substrate for poly-ubiquitination (indicated by the circles labeled with "U") and degradation by the proteasome. High levels of reporter poly-ubiquitination and/or proteasome activity result in little or no GFP fluorescence.

B Quantified fluorescence of Ub^{G76V}-GFP normalized to mRFP in the hypodermis from animals of the indicated time point (in hours) after the L4 stage. Animals have been exposed to the indicated knockdown RNAi bacterial strains or a strain that only contains the empty RNAi vector. $^*P < 0.001$, Student's *t*-test corrected for multiple comparisons at each time point using the Holm–Sidak method. $N = 20$ animals per genotype and time point. Error bars indicate SEM.

C, D Co-expression via the *col-19* promoter of Ub^{G76V}-GFP (green) and mRFP (red) in *C. elegans* hypodermis from a single integrated transgene at L4 + 48 h. Wild-type animals are shown. Scale bar, 50 μm. Ub^{G76V}-GFP fluorescence is barely detectable.

E, F Co-expression via the *sur-5* promoter of Ub^{G76V}-GFP (green) and mCherry (red) in *C. elegans* from two separate integrated transgenes (with focus on the intestine) at L4 + 48 h. Wild-type animals are shown. Scale bar, 50 μm. Ub^{G76V}-GFP fluorescence is barely detectable.

G, H Co-expression of Ub^{G76V}-GFP (green) and mRFP (red) in *C. elegans* hypodermis at L4 + 48 h in *dop-1(vs100)* mutants. Scale bar, 50 μm. Abundant, stable Ub^{G76V}-GFP fluorescence is observed.

I, J Co-expression of Ub^{G76V}-GFP (green) and mCherry (red) in *C. elegans* from the *sur-5* promoter at L4 + 48 h in *dop-1(vs100)* mutants. Scale bar, 50 μm. Abundant, stable Ub^{G76V}-GFP fluorescence is observed, particularly in the intestine.

K Quantified fluorescence of Ub^{G76V}-GFP normalized to mRFP in the hypodermis from animals of the indicated time point (in hours) after the L4 stage and of the indicated genotype. $^*P < 0.001$, Student's *t*-test corrected for multiple comparisons at each time point using the Holm–Sidak method. $N = 20$ animals per genotype and time point. Error bars indicate SEM.

L Quantified fluorescence of Ub^{G76V}-GFP normalized to mRFP in the hypodermis of animals at L4 + 48 h and of the indicated genotypes. $^{***}P < 0.001$, ANOVA with Dunnett's *post hoc* comparison to the wild-type control. $N = 20$ animals per genotype and time point. Error bars indicate SEM.

M Quantified fluorescence of Ub^{G76V}-GFP normalized to mCherry (both expressed by the *sur-5* promoter) in the intestine of animals at L4 + 48 h and of the indicated genotypes. $^{***}P < 0.001$, $^{**}P < 0.01$, $^*P < 0.05$, ANOVA with Dunnett's *post hoc* comparison to the wild-type control. $N = 20$ animals per genotype and time point. Error bars indicate SEM.

epithelial tissue types (Fig 1G–M). In addition, loss-of-function mutations in *dop-4*, the other D1-like DAR in *C. elegans*, also resulted in elevated Ub^{G76V}-GFP (Fig 1L and M). By contrast, loss of *dop-2* or *dop-3*, which encode D2-like DARs, did not affect Ub^{G76V}-GFP (Fig 1L and M). These results indicate that DA signaling promotes the degradation of unstable UPS substrates in epithelia via activation of D1-like DARs.

Dopaminergic neurons secrete DA into the pseudocoelomic body cavity where it can diffuse to multiple tissues. For example, secreted DA acts through the receptors DOP-2 and DOP-3 on motoneurons to regulate body wall muscle contraction and locomotion (Chase *et al*, 2004). We reasoned that DA might regulate Ub^{G76V}-GFP turnover in epithelia either directly (by acting through DA receptors like DOP-1 on epithelial membranes) or indirectly (by acting through DA receptors on neurons, which in turn transmit a second signal to epithelia). Previous studies of DOP-1 focused on its expression in neurons using GFP-based expression reporters (Tsalik *et al*, 2003; Chase *et al*, 2004; Sanyal *et al*, 2004). We examined transgenic animals for one of these reporters, *adEx1647*, a translational reporter that contains about 4 kb of upstream promoter sequences and about 5 kb of the coding exons and introns (almost the entire coding region) (Tsalik *et al*, 2003). We found that DOP-1, in addition to being expressed in several sets of neurons, is also expressed in adult epithelial cells, including the intestine and hypodermis (Fig EV1A and B). To address whether DOP-1 function is required cell autonomously in epithelia to regulate Ub^{G76V}-GFP turnover, we generated a transgene, $P_{vha\text{-}6}$*::dop-1(+)*, containing the *vha-6* promoter, which is specific for the intestine, and coding sequences for the wild-type *dop-1* gene. As a positive control, we also generated a complete wild-type rescuing *dop-1* transgene, called $P_{dop\text{-}1}$*::dop-1(+)*, containing the *dop-1* promoter and coding sequences. These transgenes were separately introduced into *dop-1* mutants containing the $P_{sur\text{-}5}$*::* Ub^{G76V}*-GFP*. The resulting transgenic animals were examined for fluorescence at L4 + 48 h. In contrast to *dop-1* mutants lacking either rescuing transgene, *dop-1* mutants with either $P_{dop\text{-}1}$*::dop-1 (+)* or $P_{vha\text{-}6}$*::dop-1(+)* showed wild-type levels of Ub^{G76V}-GFP turnover (Fig EV1C). These results demonstrate that DOP-1 is required cell autonomously in epithelia to regulate Ub^{G76V}-GFP turnover and support a model in which DA acts on receptors directly on epithelial cell membranes.

Dopaminergic signaling promotes protein poly-ubiquitination without perturbing proteasome function

The stabilization of Ub^{G76V}-GFP protein in DA signaling mutants could be due to either a reduction in its poly-ubiquitination or a reduction in its proteolysis by the proteasome in these mutants. To determine the molecular mechanism by which DA signaling mediates Ub^{G76V}-GFP turnover, we examined Ub^{G76V}-GFP protein by Western blot, detecting it with either anti-ubiquitin antibodies or anti-GFP antibodies (Fig 2A). We detected little Ub^{G76V}-GFP protein when it was expressed in hypodermis in wild-type animals at L4 + 48 h. In *cat-2*, *dop-1*, and *dop-4* mutants, however, we detected an increase in non-ubiquitinated, mono-ubiquitinated, and di-ubiquitinated species, suggesting that these mutants either have a reduction in initial mono-ubiquitination and subsequent poly-ubiquitin chain extension, or have reduced ability to clear ubiquitinated substrates (Fig 2A). While we did not detect proteins larger than 50 kDa in DA signaling mutants using the anti-GFP antibodies, we did detect additional proteins ranging from 50 to 80 kDa in these mutants using anti-ubiquitin antibodies. We quantified the accumulation of these proteins by conducting Western blots using anti-ubiquitin antibodies on multiple biological replicates of wild-type animals and *dop-1* mutants (Fig EV2A). While we cannot determine whether such proteins are mono-, di-, or poly-ubiquitinated, our results suggest that ubiquitinated forms of some endogenous proteins accumulate in DA signaling mutants. We also observed a similar increase in non-ubiquitinated and partially ubiquitinated proteins in these mutants when the reporter was expressed from the *sur-5* promoter, which is more broadly expressed (Fig 2B).

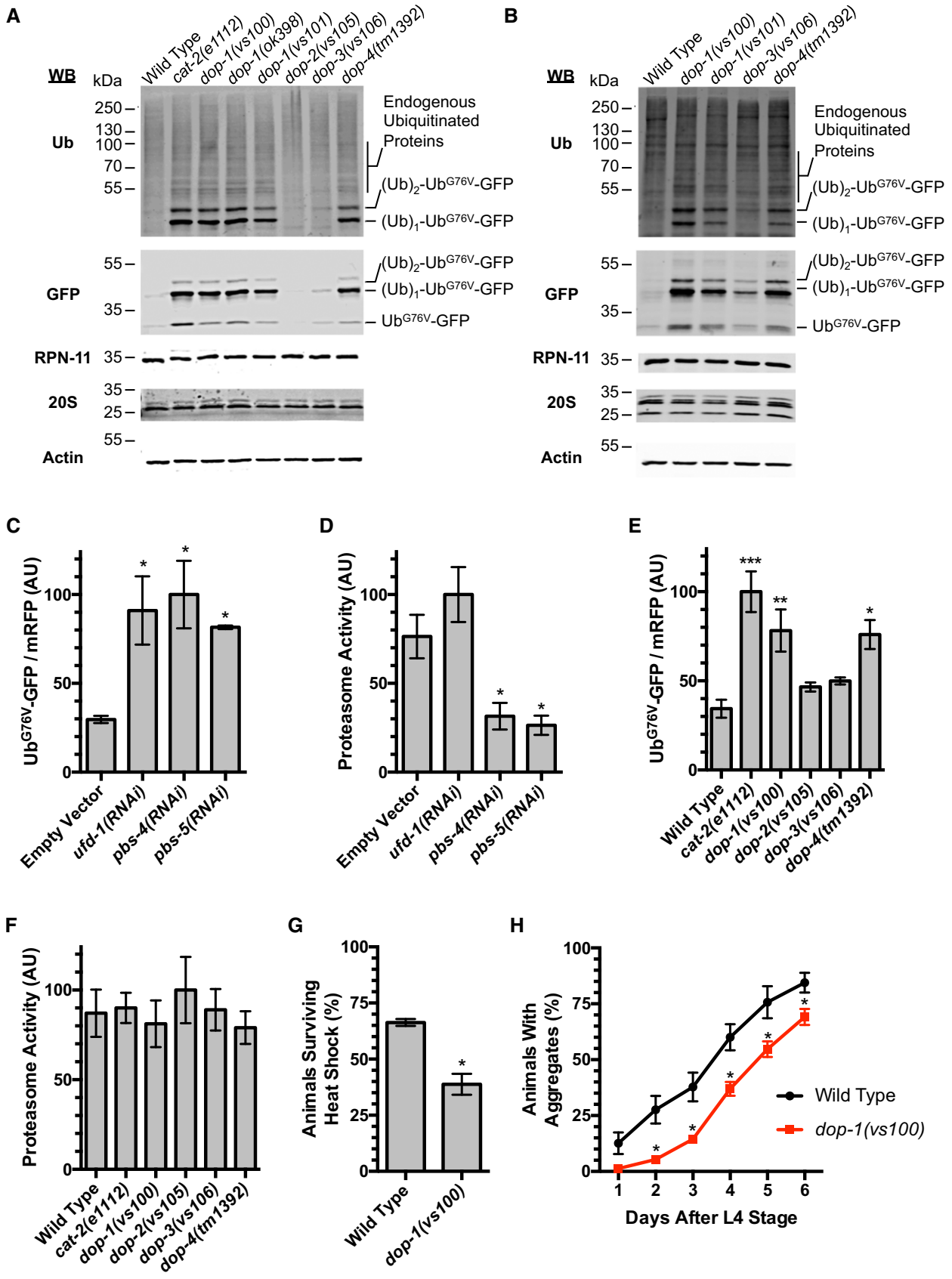
A
WB
kDa
Wild Type
cat-2(e1112)
dop-1(vs100)
dop-1(ok398)
dop-1(vs101)
dop-2(vs105)
dop-3(vs106)
dop-4(tm1392)
Ub
250
130
100
70
55
Endogenous Ubiquitinated Proteins
(Ub)2-UbG76V-GFP
(Ub)1-UbG76V-GFP
GFP
55
35
(Ub)2-UbG76V-GFP
(Ub)1-UbG76V-GFP
UbG76V-GFP
RPN-11
35
20S
35
25
Actin
55
B
WB
kDa
Wild Type
dop-1(vs100)
dop-1(vs101)
dop-3(vs106)
dop-4(tm1392)
Ub
250
130
100
70
55
Endogenous Ubiquitinated Proteins
(Ub)2-UbG76V-GFP
(Ub)1-UbG76V-GFP
GFP
55
35
(Ub)2-UbG76V-GFP
(Ub)1-UbG76V-GFP
UbG76V-GFP
RPN-11
35
20S
35
25
Actin
55
C
UbG76V-GFP / mRFP (AU)
100
50
0
Empty Vector
ufd-1(RNAi)
pbs-4(RNAi)
pbs-5(RNAi)
D
Proteasome Activity (AU)
100
50
0
Empty Vector
ufd-1(RNAi)
pbs-4(RNAi)
pbs-5(RNAi)
E
UbG76V-GFP / mRFP (AU)
100
50
0
Wild Type
cat-2(e1112)
dop-1(vs100)
dop-2(vs105)
dop-3(vs106)
dop-4(tm1392)
F
Proteasome Activity (AU)
100
50
0
Wild Type
cat-2(e1112)
dop-1(vs100)
dop-2(vs105)
dop-3(vs106)
dop-4(tm1392)
G
Animals Surviving Heat Shock (%)
100
75
50
25
0
Wild Type
dop-1(vs100)
H
Animals With Aggregates (%)
100
75
50
25
0
1
2
3
4
5
6
Days After L4 Stage
Wild Type
dop-1(vs100)

Figure 2.

Figure 2. Dopaminergic signaling promotes protein poly-ubiquitination.

A Western blot of lysed nematodes at the L4 + 48 h stage, probed with antibodies recognizing ubiquitin, GFP, RPN-11, multiple 20S proteasome subunits, or actin as a loading control. Animals express Ub^{G76V}-GFP protein in their hypodermis. The position of molecular weight markers is shown on the left of each blot. The position of Ub^{G76V}-GFP protein, as well as Ub^{G76V}-GFP with the indicated number of additional ubiquitin moieties, based on molecular weight, is indicated on the right of each blot. Twenty animals were loaded per lane for each indicated genotype (WT indicates wild type).

B Western blot of lysed nematodes at the L4 + 48 h stage, probed and annotated as in (A). Animals express Ub^{G76V}-GFP protein from the *sur-5* promoter. Thirty animals were loaded per lane for each indicated genotype.

C Quantified fluorescence of Ub^{G76V}-GFP normalized to mRFP from lysates of transgenic nematodes at L4 + 48 h that express these reporters in the hypodermis. Animals were exposed to bacteria containing the indicated RNAi clone or an empty RNAi vector as a control. $*P < 0.05$, ANOVA with Dunnett's *post hoc* comparison to the empty RNAi vector control. $N = 3$ trials. Error bars indicate SEM.

D Quantified epoxomicin-sensitive proteasome activity (as measured through the turnover of fluorescent chymotrypsin substrate) from the same lysates as in (C). $*P < 0.05$, ANOVA with Dunnett's *post hoc* comparison to the empty RNAi vector control. $N = 3$ trials. Error bars indicate SEM.

E Quantified fluorescence of Ub^{G76V}-GFP normalized to mRFP from lysates of transgenic nematodes at L4 + 48 h that express these reporters in the hypodermis. Animals were of the indicated genotype. $***P < 0.001$, $**P < 0.01$, $*P < 0.05$, ANOVA with Dunnett's *post hoc* comparison to wild type. $N = 4$ trials. Error bars indicate SEM.

F Quantified epoxomicin-sensitive proteasome activity (as measured through the turnover of fluorescent chymotrypsin substrate) from the same lysates as in (E). No statistical difference ($P < 0.05$ cutoff) was detected by ANOVA. $N = 4$ trials. Error bars indicate SEM.

G Percentage of live animals of the indicated genotype assayed after 6-h exposure to heat shock. 100% of control animals of the same genotype but not given heat shock survived. $*P < 0.01$, Student's *t*-test. $N = 3$ trials. Error bars indicate SEM.

H Percent of animals of the indicated genotype containing aggregates of $Poly(Q)_{44}$::YFP at the indicated time (in days) after L4 stage. $*P < 0.01$, Student's *t*-test. $N = 3$ trials, 50–80 animals per trial per day. Error bars indicate SEM.

Source data are available online for this figure.

Together, these results suggest that DA signaling is required for normal levels of either protein ubiquitination, proteolysis by the proteasome, or both.

We also directly examined the proteasome in DA signaling mutants. We did not observe changes in the levels of proteasome subunits in lysates for various DA signaling mutants (Fig 2A and B). To directly assay proteasome activity, we generated lysates of L4 + 48 h nematodes that express Ub^{G76V}-GFP in the hypodermis. We first analyzed Ub^{G76V}-GFP and mRFP levels in these lysates by fluorescence spectroscopy (Fig 2C). We observed low levels of Ub^{G76V}-GFP at L4 + 48 h in wild-type animals using this approach, similar to what we observed by epifluorescence microscopy and Western blot analysis. We also generated lysates from animals exposed to RNAi bacteria, including animals knocked down for the E4 poly-ubiquitination chain extending enzyme *ufd-1*, as well as for the proteasome subunits *pbs-4* and *pbs-5*. Exposure to RNAi against any of these genes resulted in stabilized Ub^{G76V}-GFP (Fig 2C). We incubated the same lysates with the fluorescent chymotryptic substrate Suc-Leu-Leu-Val-Tyr-AMC in the presence or absence of the proteasome inhibitor epoxomicin to measure proteasome activity over time. As expected, RNAi knockdown of *pbs-4* and *pbs-5* resulted in diminished proteasome activity relative to an empty RNAi vector control (Fig 2D). By contrast, RNAi knockdown of *ufd-1*, a gene that normally promotes poly-ubiquitination of substrates but is not involved in proteasome catalytic activity, as expected did not reduce proteasome activity. These findings indicate that about a threefold decrease in proteasome activity results in about a threefold increase in Ub^{G76V}-GFP levels in this assay.

We next generated lysates from multiple DA signaling mutants. Similar to what we observed by epifluorescence microscopy and Western blot analysis, we found that *cat-2*, *dop-1*, and *dop-4* mutants have elevated levels of Ub^{G76V}-GFP protein (Fig 2E). We performed the same analysis of proteasome activity in lysates from these mutants; however, we did not observe a substantial change in proteasome activity in any of these mutants (Fig 2F). If the accumulation of Ub^{G76V}-GFP in DA signaling mutants were due to a decrease in proteasome activity, then we should have (i) observed an increase in poly-ubiquitinated (i.e., 4 or more ubiquitin moieties) Ub^{G76V}-GFP relative to total Ub^{G76V}-GFP in these mutants, and (ii) detected a healthy decrease in our direct measurement of proteasome activity. Instead, the observed decrease in poly-ubiquitinated proteins and the unchanged activity in our proteasome assay strongly suggest that DA signaling does not regulate proteasome activity.

If DA signaling promotes the turnover of Ub^{G76V}-GFP through increased poly-ubiquitination instead of increased proteasome activity, then a knockdown of proteasome subunits should further enhance the stability of Ub^{G76V}-GFP in *dop-1* mutants. We examined Ub^{G76V}-GFP by Western blot in wild-type and in *dop-1* mutants either exposed to empty RNAi vector or *pbs-5*(*RNAi*). Wild-type animals accumulate mono-ubiquitinated, di-ubiquitinated, and poly-ubiquitinated Ub^{G76V}-GFP when the proteasome is impaired by *pbs-5* RNAi-mediated knockdown (Fig EV2B). Knockdown of *pbs-5* in *dop-1* mutants resulted in a dramatic additive increase in poly-ubiquitinated Ub^{G76V}-GFP, demonstrating that the proteasome remains active and degrades any residual poly-ubiquitinated Ub^{G76V}-GFP in *dop-1* mutants. Taken together, our results suggest that the proteasome is not the prime target of regulation by DA. Instead, DA signaling is required for the proper ubiquitination of unstable proteins like Ub^{G76V}-GFP.

We performed two additional tests to detect changes in protein homeostasis in *dop-1* mutants. First, we examined the sensitivity of *dop-1* mutants to heat shock. After exposing adult nematodes to a 6-h heat shock (34°C), we found that nearly 70% of wild-type animals survived, whereas only about a third of *dop-1* mutant adults survived (Fig 2G), suggesting that *dop-1* mutants are less able to handle the unfolded protein burden generated by heat-shock stress. Second, we examined a polyglutamine protein aggregation reporter expressed in the intestine from the transgene $P_{vha\text{-}6}$*::Poly(Q)44::YFP* (Mohri-Shiomi & Garsin, 2008). Polyglutamine proteins form aggregates as *C. elegans* age, and this process, which is thought to be protective, is facilitated by poly-ubiquitination (Morley *et al*, 2002;

Hsu *et al*, 2003; Howard *et al*, 2007; Mohri-Shiomi & Garsin, 2008; Kirkin *et al*, 2009). We found that *dop-1* mutants were less efficient at sequestering polyglutamine proteins into these aggregates during aging (Fig 2H). Taken together, the observed impairment of protein homeostasis in *dop-1* mutants is consistent with a role for DA signaling in promoting healthy proteostasis.

Dopamine signaling promotes protein turnover via the xenobiotic stress pathway

Dopamine signaling can regulate cellular physiology through a combination of transcriptional and posttranscriptional regulatory steps (Kebabian *et al*, 1972; Cooper *et al*, 1986; Cadet *et al*, 2010). To begin to understand the mechanism of DA action with regard to proteostasis, we compared the mRNA expression profile of *dop-1* mutants to wild-type animals during adulthood (L4 + 48 h) using RNA-seq. We isolated poly-A(+) RNA from three replicates of each genotype and subjected each sample to RNA-seq. We assessed differential gene expression between genotypes using EdgeR and an FDR-adjusted *q*-value (Anders & Huber, 2010), focusing only on genes with significant changes ($q < 0.01$). As expected, the levels of Ub^{G76V}-GFP and mRFP mRNA did not vary between wild-type and *dop-1* mutants (Fig 3A). We found that 334 genes were significantly downregulated at least 1.5-fold in *dop-1* compared to wild type, whereas 436 genes were upregulated in *dop-1* relative to wild type (Table EV1). We used DAVID functional annotation clustering enrichment analysis (Da Huang *et al*, 2009a,b) on the genes regulated by DOP-1 signaling (Table EV2). Particularly striking in the set of genes that were downregulated in *dop-1* mutants compared to wild type was the enrichment of annotation clusters for genes involved in xenobiotic and endobiotic detoxification and metabolism (Lindblom & Dodd, 2006), including oxidoreductase activity (multiple CYP or cytochrome P450 enzymes), lipid modification, and glycosyl transferases (multiple UGT or UDP-glucuronosyltransferases) (Table 1). These results suggest that DA signaling through the DOP-1 receptor promotes xenobiotic detoxification.

We also noted that there were annotation clusters of genes that were upregulated in *dop-1* mutants compared to wild type and that these included C-lectins and heat-shock chaperones (Table 1). The elevated level of heat-shock gene expression in *dop-1* mutants even at permissive temperatures (20°C) suggests that DA signaling is needed to prevent a heat-shock response, which is consistent with impaired proteostasis in these mutants. The elevated levels of heat-shock genes in *dop-1* mutants are not likely to be the cause of Ub^{G76V}-GFP stabilization in those mutants because RNAi knockdown of those genes, including *hsp-4*, *hsp-16.2*, *hsp-16.11*, *hsp-16.41*, *hsp-16.48*, *hsp-16.49*, *hsp-17*, and *hsp-43*, did not suppress the stabilization of Ub^{G76V}-GFP in *dop-1* mutants: All *dop-1* animals exposed to RNAi knockdown for these genes resembled *dop-1* mutants given empty vector RNAi, with nearly all animals showing Ub^{G76V}-GFP fluorescence at L4 + 48 h. Indeed, loss-of-function mutations in the chaperones *hsp-16.2* and *hsp-43*, as well as the heat-shock transcriptional regulator *hsf-1*, in an otherwise wild-type background resulted in Ub^{G76V}-GFP stabilization, suggesting that impaired heat-shock proteostasis is sufficient to block Ub^{G76V}-GFP turnover (Fig EV3A).

Given the decreased expression of multiple xenobiotic detoxification genes in the absence of DA signaling (Fig 3A), we hypothesized that the changes in Ub^{G76V}-GFP stability in DA signaling mutants might be due to impaired xenobiotic detoxification. We tested this idea by knocking down the expression of individual candidate genes from our RNA-seq analysis using RNAi and examining the effect on Ub^{G76V}-GFP levels. We found that the knockdown of multiple CYP and UGT genes resulted in the stabilization of Ub^{G76V}-GFP in the hypodermis (Fig 3B) and the intestine (Fig 3C) relative to internal controls (mRFP and mCherry, respectively). We also examined the sensitivity to heat shock of animals knocked down for CYP and UGT genes. After a 6-h heat shock (34°C), we found a significant reduction in the number of surviving animals knocked down by RNAi for *ugt-3*, *ugt-11*, and *cyp-34A7* compared to an empty vector control (Fig 3D), suggesting that animals lacking the activity of these xenobiotic stress genes are less able to handle heat-shock stress. These results suggest that the turnover of unstable Ub^{G76V}-GFP protein and cellular UPS activity is modulated by the levels of xenobiotic detoxification enzymes, and that DA signaling, at least in part, modulates proteostasis in epithelia by promoting xenobiotic metabolism.

Given the large number of CYP and UGT genes in the genome, we were concerned that there might be a fair amount of functional redundancy between the xenobiotic detoxification components that might preclude observing a full phenotype in any single RNAi experiment. We reasoned that mutants for known master regulators of these genes might represent a more comprehensive impairment of the xenobiotic response. Xenobiotic stress response genes contribute to innate immunity against bacterial pathogens (Papp *et al*, 2012; Runkel *et al*, 2013; Pellegrino *et al*, 2014; Pukkila-Worley *et al*, 2014), and many of these genes are also regulated as part of the oxidative stress response (mediated by the SKN-1/Nrf2 transcription factor) and the insulin signaling system (mediated by the DAF-16/FOXO transcription factor) (An & Blackwell, 2003; Murphy *et al*, 2003; Oliveira *et al*, 2009; Park *et al*, 2009; Mair *et al*, 2011). Indeed, DAF-16 ChIP-seq sites are located at nearly all of the CYP and UGT genes in our RNA-seq dataset, and *cyp-34A7* was identified as a positive transcriptional target of DAF-16 through microarray analysis (Murphy *et al*, 2003). Many are also regulated by cAMP signaling and the CRH-1/CREB transcription factor, which acts downstream of DA signaling for its role in behavior modulation (Cadet *et al*, 2010; Beaulieu & Gainetdinov, 2011; Mair *et al*, 2011; Suo & Ishiura, 2013). Xenobiotic genes are also regulated by the GATA transcription factor ELT-3, with ChIP-seq sites for ELT-3 near *ugt-3*, *ugt-8*, *ugt-11*, *ugt-63*, *cyp-25A1*, *cyp-29A2*, *cyp-34A7*, and *cyp-34A8* (Budovskaya *et al*, 2008). ChIP-seq sites for the transcription factors NHR-28 and PQM-1 are also found at nearly every CYP and UGT gene identified in our RNA-seq analysis (Miyabayashi *et al*, 1999; Gerstein *et al*, 2010; Tepper *et al*, 2013; Araya *et al*, 2014), suggesting that these might be additional regulators of the xenobiotic stress response genes.

We examined Ub^{G76V}-GFP levels in loss-of-function mutants for *skn-1*, *daf-16*, the two *C. elegans* CREB genes (*crh-1* and *crh-2*), *elt-3*, *nhr-28*, and *pqm-1*. We found that Ub^{G76V}-GFP was stabilized in each case (Figs 3E and EV3B), suggesting that broad regulators of the xenobiotic stress response and the detoxification pathway are required for Ub^{G76V}-GFP turnover. The effects of *cat-2* and *let-3* mutations on Ub^{G76V}-GFP turnover are not additive, as double mutants showed similar levels of stabilization relative to single mutants (Fig EV3C), consistent with these genes acting in the same

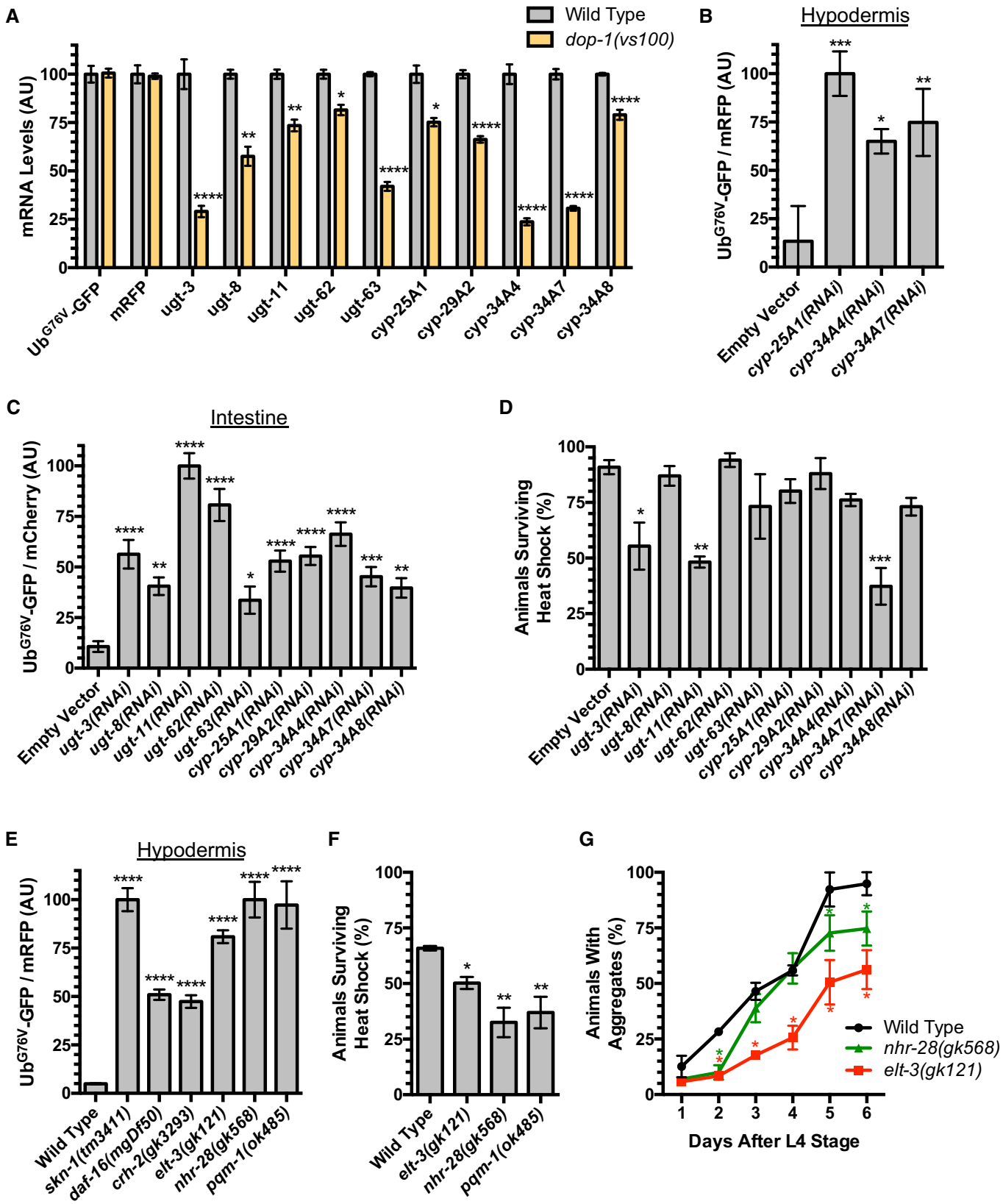

Figure 3.

Figure 3. Dopamine signaling promotes protein turnover via the xenobiotic stress pathway.

A Relative abundance of mRNA for the indicated xenobiotic stress response gene (or Ub^{G76V}-GFP or mRFP) detected in wild-type versus *dop-1* mutants. Values are based on RNA-seq/EdgeR analysis, with the relative levels for each gene normalized to the value observed in the wild-type control. ****$P < 0.0001$, **$P < 0.01$, *$P < 0.05$, FDR from EdgeR analysis using a Benjamini and Hochberg correction. Error bars indicate SEM.

B, C Quantified fluorescence of Ub^{G76V}-GFP normalized to (B) mRFP in the hypodermis or (C) mCherry in the intestine from L4 + 48 h animals exposed to feeding RNAi for either an empty vector control or the indicated xenobiotic stress gene. ****$P < 0.0001$, ***$P < 0.001$, **$P < 0.01$, *$P < 0.05$, ANOVA, Tukey's multiple comparison test compared to control. $N = 20$ animals per genotype and time point. Error bars indicate SEM.

D Percentage of live animals raised on the indicated feeding RNAi (or empty vector control) bacteria assayed after 6-h exposure to heat shock. 100% of control animals of the same genotype but not given heat shock survived. ***$P < 0.001$, **$P < 0.01$, *$P < 0.05$, ANOVA, Tukey's multiple comparison test compared to wild type. $N = 3$ trials. Error bars indicate SEM.

E Quantified fluorescence of Ub^{G76V}-GFP normalized to mRFP in the hypodermis from L4 + 48 h animals of the indicated genotype. ****$P < 0.0001$, ANOVA, Tukey's multiple comparison test compared to wild type. $N = 20$ animals per genotype and time point. Error bars indicate SEM.

F Percentage of live animals of the indicated genotype assayed after 6-h exposure to heat shock. 100% of control animals of the same genotype but not given heat shock survived. **$P < 0.01$, *$P < 0.05$, ANOVA, Tukey's multiple comparison test compared to wild type. $N = 3$ trials. Error bars indicate SEM.

G Percent of animals of the indicated genotype containing aggregates of $Poly(Q)_{44}$::YFP at the indicated time (in days) after L4 stage. *$P < 0.001$, Student's *t*-test corrected for multiple comparisons at each time point using the Holm–Sidak method. $N = 3$ trials, 50–80 animals per trial per day. Error bars indicate SEM.

genetic pathway. Consistent with Ub^{G76V}-GFP stabilization in these mutants, *daf-16* mutants are sensitive to heat shock (Saul *et al*, 2008), and *skn-1* knockdown by RNAi results in impairment of UPS activity and elevated levels of heat-shock proteins (Saul *et al*, 2008). We also examined *elt-3*, *nhr-28*, and *pqm-1* mutants for sensitivity to heat shock, finding a significant reduction in the number of surviving animals in these mutants compared to wild type after a 6-h heat shock (34°C) (Fig 3F), suggesting that they are less able to handle heat-shock stress. We also introduced the $P_{vha\text{-}6}$*::Poly(Q)44::YFP* into *elt-3* and *nhr-28* mutants (the reporter was too closely linked to *pqm-1* for analysis in *pqm-1* mutants) and found that these mutants were less efficient at sequestering polyglutamine proteins into aggregates (Fig 3G). Taken together, our results indicate that master regulators of the xenobiotic stress response are required for proper proteostasis.

Table 1. DAVID functional annotation clustering enrichment analysis for genes regulated by DOP-1 signaling.

Annotation cluster	Cluster enrichment score	Cluster EASE score *P*-value
Genes that are downregulated in *dop-1* mutants		
Collagens and cuticle formation	9.60	2.5×10^{-10}
Oxidoreductase activity and cytochrome P450s	3.73	1.9×10^{-4}
Uncharacterized *C. elegans* proteins	2.35	4.5×10^{-3}
UDP-glucuronosyltransferases	2.22	6.0×10^{-3}
Extracellular protease inhibitors	2.11	7.8×10^{-3}
Genes that are upregulated in *dop-1* mutants		
Hedgehog receptor signaling	3.49	3.2×10^{-4}
C-lectins	2.73	1.9×10^{-3}
Heat-shock proteins	2.26	5.5×10^{-3}

Individual annotation clusters generated by DAVID functional clustering are listed for genes that are downregulated (top half of table) and upregulated (bottom half of table) in *dop-1* mutants relative to wild type. The cluster enrichment score is the geometric mean (in –log scale) of the *P*-values (from Fisher's exact test with DAVID EASE Score modification, also shown) of all of the individual annotations within that cluster.

Mechanosensory dopaminergic neurons are required to modulate protein turnover in epithelia

Mechanosensory neurons release DA in response to shear stress on the body wall as nematodes enter high-viscosity bacterial lawns (Sawin *et al*, 2000; Kindt *et al*, 2007). Given that DA signaling promotes the expression of xenobiotic stress response genes, we reasoned that such signaling might be (i) activated by pathogenic bacteria and (ii) required for animals to survive pathogenic infection. To explore this possibility, we first tested whether mechanosensation is required to modulate Ub^{G76V}-GFP turnover in epithelial tissues by examining mutants lacking *mec-5*, a unique collagen required for all mechanosensation in the nematode, and *trp-4*, a mechanosensory TRPN (NOMPC) channel expressed and required specifically in the mechanosensory dopaminergic neurons (Du *et al*, 1996; Emtage *et al*, 2004; Li *et al*, 2006; Kang *et al*, 2010). We found that Ub^{G76V}-GFP turnover is reduced in *mec-5* and *trp-4* mutants (Figs 4A and EV3D), although not to the same extent as in DA signaling mutants, indicating that the activation of these neurons by environmental mechanical stimulation is required to fully promote Ub^{G76V}-GFP turnover in epithelia, but that these dopaminergic neurons might also promote Ub^{G76V}-GFP turnover in response to additional environmental cues besides mechanical stimulation.

TRP-4 is expressed primarily in dopaminergic neurons (ADE, CEP, PDE), but it is also found in the neurons DVA and DVC. To determine whether the dopaminergic neurons specifically are required to promote Ub^{G76V}-GFP turnover in epithelia, we took advantage of a transgene, $P_{dat\text{-}1}$*::trp-4(d)*, that expresses a toxic TRP-4 mutant channel under the control of the *dat-1* promoter and is thus only active in dopaminergic neurons (Nagarajan *et al*, 2014). The transgene triggers a progressive cell death of the dopaminergic neurons but not DVA or DVC. We introduced this transgene into nematodes that express Ub^{G76V}-GFP and found that Ub^{G76V}-GFP turnover was reduced (Fig 4A). The magnitude of the effect caused by $P_{dat\text{-}1}$*::trp-4(d)* was not to the same extent as that observed in DA signaling mutants; however, not all of dopaminergic neurons undergo neurodegeneration in many of the $P_{dat\text{-}1}$*::trp-4(d)* transgenic animals (Nagarajan *et al*, 2014), so a partial phenotype

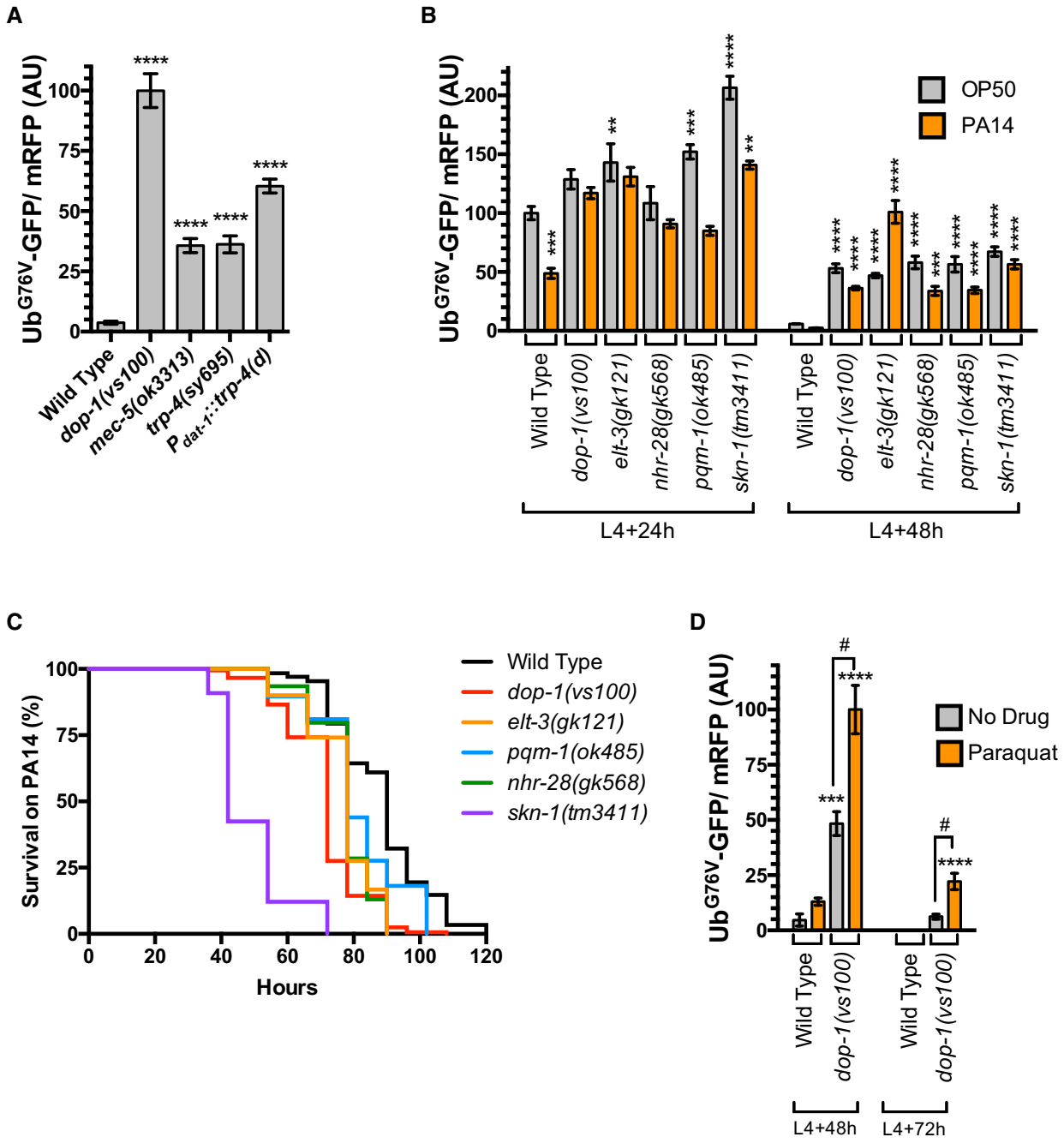

Figure 4. Dopamine signaling modulates xenobiotic stress survival.

A Quantified fluorescence of Ub^{G76V}-GFP normalized to mRFP in the hypodermis from L4 + 48 h animals of the indicated genotype. ****$P < 0.0001$, ANOVA, Tukey's multiple comparison test compared to wild type. $N = 20$ animals per genotype. Error bars indicate SEM.

B Quantified fluorescence of Ub^{G76V}-GFP normalized to mRFP in the hypodermis from either L4 + 24 h animals (left half of graph) or L4 + 48 h animals (right half of graph) of the indicated genotype. Animals were either continually grown on regular OP50 food (gray bars) or switched to PA14 food at the L4 stage (orange bars). ****$P < 0.0001$, ***$P < 0.001$, **$P < 0.01$, ANOVA, Tukey's multiple comparison test compared to wild type. $N = 20$ animals per genotype. Error bars indicate SEM.

C Survival curves (percentage of live animals assayed each hour after PA14 exposure) for the indicated mutants at 20°C. $P_{log\text{-}rank} < 0.0001$. Median survival time was 90 h for wild type ($N = 304$), 72 h for *dop-1(vs100)* ($N = 180$), 78 h for *elt-3(gk121)* ($N = 120$), 78 h for *pqm-1(ok485)* ($N = 116$), 78 h for *nhr-28(gk568)* ($N = 123$), and 42 h for *skn-1(tm3411)* ($N = 33$). Eight wild-type animals and six *dop-1* mutants were censored (the animals crawled up the side of the plate and dessicated). The media contained 50 μg/ml of 5-fluoro-2′-deoxyuridine (FUdR) to prevent the growth of egg offspring during the experiment.

D Quantified fluorescence of Ub^{G76V}-GFP normalized to mRFP in the hypodermis from either L4 + 48 h animals (left half of graph) or L4 + 72 h animals (right half of graph) of the indicated genotype. Animals were either continually grown on regular OP50 food (gray bars) or switched to NGM plates containing 1 mM paraquat at the L4 stage (orange bars). ****$P < 0.0001$, ***$P < 0.001$, ANOVA, Tukey's multiple comparison test compared to wild type. #$P < 0.001$, ANOVA, Bonferroni multiple comparison as indicated by the bracketed lines. $N = 20$ animals per genotype. Error bars indicate SEM. No Ub^{G76V}-GFP fluorescence was detected in wild type at L4 + 72 h on NGM plates containing either 1 mM paraquat or no drug at all.

relative to DA signaling mutants is expected. Taken together, our results show that the dopaminergic neurons are required non-autonomously to regulate the turnover of unstable proteins like Ub^{G76V}-GFP in epithelia.

Xenobiotic stress modulates protein turnover via dopamine-dependent mechanism

We next tested whether exposure to a different type of bacteria—in this case the pathogenic PA14 strain of *Pseudomonas aeruginosa*—results in altered Ub^{G76V}-GFP turnover compared to the standard, non-pathogenic OP50 *E. coli* feeding strain. We found that Ub^{G76V}-GFP levels relative to mRFP control were depressed (even at the earlier L4 + 24 h time point) in nematodes that were switched to PA14 lawns beginning at the L4 stage compared to those grown continually on OP50 (Fig 4B), suggesting that the ability of epithelial cells to remove unstable proteins like Ub^{G76V}-GFP is enhanced in nematodes exposed to PA14 bacteria. Mutations in *dop-1* blocked the elevated turnover of Ub^{G76V}-GFP at L4 + 24 h, as well as at later time points (Fig 4B). In addition, loss-of-function mutations in the xenobiotic stress regulators *elt-3*, *nhr-28*, and *pqm-1*, as well as a mutation in *skn-1*, which also depresses xenobiotic stress response gene expression and impairs innate immunity against bacterial pathogens (An & Blackwell, 2003; Oliveira *et al*, 2009; Park *et al*, 2009; Papp *et al*, 2012), all blocked Ub^{G76V}-GFP turnover (Fig 4B). These results indicate that pathogenic bacteria like PA14 can promote the turnover of unstable proteins through a process that requires DA signaling and most likely the xenobiotic stress response. These results are consistent with previous observations that the specific strain of the bacterial food source can influence proteostasis and protein poly-ubiquitination in feeding nematodes (Segref *et al*, 2011); however, unlike the variant non-pathogenic *E. coli* strains used in the previous study, which reduced Ub^{G76V}-GFP turnover, we find that pathogenic *P. aeruginosa* triggers accelerated turnover.

If DA signaling mediates a xenobiotic defense response, then one would expect that loss-of-function mutants for either DA signaling components or regulators of the xenobiotic defense response should show increased sensitivity to bacterial infection. We examined this idea by quantifying nematode survival on lawns of PA14 over time. Wild-type nematodes begin to succumb to PA14 after about 70 h of exposure, with most animals dying after about 110 h (Fig 4C). We confirmed that mutants for *skn-1* die more rapidly (Fig 4C) when exposed to PA14 (Papp *et al*, 2012). Similarly, we found that mutants for *dop-1, elt-3, pqm-1,* and *nhr-28* succumbed to PA14 more quickly than did wild type, although not quite at the rapid rate of *skn-1* mutants, indicating that DA signaling and regulators of the xenobiotic stress response are required for effective survival to pathogen exposure.

If the xenobiotic stress response is required for efficient Ub^{G76V}-GFP turnover, then one can infer that xenobiotic toxins and ROS impair cellular proteostasis, particularly proteostasis maintained by the UPS. Indeed, Ub^{G76V}-GFP turnover is sensitive to a variety of xenobiotic compounds and ROS, including ethanol, cadmium, and paraquat (Segref *et al*, 2011). We examined Ub^{G76V}-GFP levels in the hypodermis of either untreated animals or animals treated with 1 mM paraquat (Fig 4D). Paraquat treatment only generated a minor increase in Ub^{G76V}-GFP levels in the hypodermis of wild-type animals. By contrast, paraquat treatment resulted in a twofold increase in Ub^{G76V}-GFP in *dop-1* mutants at L4 + 48 h and persistent Ub^{G76V}-GFP stabilization even out to L4 + 72 h. These results are consistent with the reduced levels of xenobiotic stress response genes in *dop-1* mutants and suggest that DA signaling is required to protect the epithelial proteome from ROS and xenobiotic toxins. Taken together, our findings suggest that DA signaling promotes healthy proteostasis through activation of the xenobiotic stress response in frontline barrier epithelia, and that this regulation is critical for innate immunity against invading pathogens.

Discussion

In previous studies, the GFP-based UPS substrate Ub^{G76V}-GFP was expressed from transgenes and employed as a reporter for UPS activity (Dantuma *et al*, 2000; Lindsten *et al*, 2003; Liu *et al*, 2011; Segref *et al*, 2011). In *C. elegans*, Ub^{G76V}-GFP undergoes regular turnover when expressed in epithelial cells of either the intestine or the hypodermis, and this turnover is enhanced as animals enter peak fecundity. Here, we have used this reporter to screen for modulators of UPS activity (and by extension proteostasis) in epithelia. We found that the dopamine signaling system, including the D1-like receptors DOP-1 and DOP-4, promotes healthy proteostasis and innate immunity by driving the expression of xenobiotic detoxification genes, the activity of which is required to remove xenobiotic compounds and ROS to prevent their impairment of the proteome. Mechanosensory neurons release dopamine in response to environmental viscosity, which is a hallmark of bacterial growth. Nematodes appear to use dopaminergic sensory neurons to sense the bacterial environment for potential pathogens, with the resulting neurohormone signaling in turn modulating proteostasis in epithelial barrier tissues in preparation for possible infection. These conclusions are supported by several pieces of data. First, in the absence of dopamine signaling, a UPS reporter shows depressed turnover in intestine and hypodermis. Second, in the absence of dopamine signaling, there are no detectable changes in proteasome activity, but there is a detectable increase in the fraction of non-ubiquitinated proteins and lower mobility poly-ubiquitinated proteins, suggesting that dopamine signaling mutants have impaired mono- and poly-ubiquitination rather than impaired proteasome proteolysis activity. Third, in the absence of dopamine signaling, the levels of multiple xenobiotic detoxification enzymes are reduced. Fourth, RNAi knockdown of these individual xenobiotic detoxification enzymes results in reduced UPS reporter turnover, as does reduction of function in master regulators (*crh-1*, *crh-2*, *skn-1*, *daf-16, elt-3, nhr-28,* and *pqm-1*) of the xenobiotic detoxification response. Fifth, mutations that either impair touch sensation alone in the dopaminergic sensory neurons or kill these neurons outright are sufficient to reduce the turnover of the UPS reporter in epithelia. Sixth, growth on pathogenic bacteria accelerates UPS reporter turnover, and this acceleration requires dopaminergic signaling. Seventh, exposure of nematodes to the ROS generating agent paraquat results in dramatic UPS reporter stabilization when dopaminergic signaling is impaired. Finally, mutations that impair dopaminergic signaling reduce the ability of nematodes to survive pathogenic infection and proteotoxic insult. Taken together, our findings demonstrate that mechanosensory dopaminergic neurons

respond to environmental cues and use dopamine as a neurohormone to enhance the ability of frontline epithelial barrier cells to counter potential infection and protein damage.

Modulation of proteostasis by DA signaling likely complements the role of DA signaling in modulating behavior. Multiple published studies demonstrated that *C. elegans* employ their mechanosensory dopaminergic neurons to sense viscous bacterial lawns and release DA as a long-distance neurohormone (Sawin *et al*, 2000; Chase *et al*, 2004; Kindt *et al*, 2007; Suo & Ishiura, 2013). DA acts through D2-like receptors on the motoneurons to slow locomotion so as to facilitate feeding on the newly identified potential food source (Chase *et al*, 2004; Suo & Ishiura, 2013). We propose that DA simultaneously acts through D1-like receptors to activate expression of xenobiotic detoxification genes and modulate protein homeostasis in epithelia (Fig EV4). Infection by pathogenic bacteria results in protein damage in barrier epithelia (Mohri-Shiomi & Garsin, 2008). It is therefore reasonable that a multicellular organism like *C. elegans* might evolve the ability to sense bacteria and translate such sensation into a neurohormonal signal to activate mechanisms to counteract potential damage. Thus, this sensory-based signaling mechanism, in addition to activating feeding behaviors in response to a potential bacterial food source, would also prepare the animal in case the food source turns out to be pathogenic. This touch-based mechanism likely complements other sensory mechanisms that trigger an innate immunity response (Chang *et al*, 2011; Aballay, 2013; Meisel *et al*, 2014; Mardones *et al*, 2015).

Dopamine signaling is likely to act through CREB to promote the xenobiotic stress response. DA signaling regulates changes in gene expression through the transcription factor CREB, and the *C. elegans* CREB homolog CRH-1 promotes the expression of xenobiotic detoxification genes (Mair *et al*, 2011; Suo & Ishiura, 2013). We found that mutations in the CREB homologs *crh-1* and *crh-2* result in reduced UPS activity, similar to that observed in DA signaling mutants. The Nrf2 homolog SKN-1 also promotes the expression of xenobiotic detoxification genes and plays an important role in innate immunity (Inoue *et al*, 2005; Oliveira *et al*, 2009; Park *et al*, 2009; Choe *et al*, 2012; Papp *et al*, 2012). Mutations in *skn-1* also result in reduced UPS reporter turnover, but whether DA signaling acts through SKN-1 remains unknown. The transcription factors DAF-16, ELT-3, NHR-28, and PQM-1 also regulate xenobiotic detoxification and also show stabilized UPS reporter protein, as does direct xenobiotic compound and ROS exposure, lending further support for the xenobiotic detoxification response as a proteostasis mechanism (Miyabayashi *et al*, 1999; Murphy *et al*, 2003; Budovskaya *et al*, 2008; Gerstein *et al*, 2010; Segref *et al*, 2011; Tepper *et al*, 2013; Araya *et al*, 2014). It will be interesting to determine whether DA signaling also acts through these transcription factors.

We previously observed that EGF signaling regulates the timing of Ub^{G76V}-GFP turnover in the hypodermis, raising the possibility that DA signaling might act through EGF signaling (Liu *et al*, 2011). We think that this is unlikely, however, because mutants for EGF signaling and DA signaling have distinct gene expression profiles (EGF signaling does not regulate the same set of xenobiotic response genes as does DA signaling). Interestingly, we tried to generate double mutants between gain-of-function *let-23* EGF receptor mutations, which result in accelerated protein turnover, and *dop-1* loss-of-function mutations, which result in depressed protein turnover; however, we were not able to obtain viable double mutants, suggesting that these two pathways might act independently from one another and complement one another.

How the xenobiotic detoxification network in turn modulates UPS activity and proteostasis remains to be elucidated, but the simplest explanation might be that xenobiotic modification of cellular proteins increases their availability as poly-ubiquitination substrates, most likely by damaging them. When confronted by xenobiotic toxin exposure, the increase in damaged and unfolded protein load might be so high that the UPS machinery required to remove them becomes saturated unless DA signaling is present to activate the xenobiotic stress response to prevent the toxins from reaching the proteome. We believe that in the absence of DA signaling, the multiple E3 and E4 ubiquitin ligases involved in removing damaged proteins become saturated rather than the proteasome because (i) non-ubiquitinated, mono-ubiquitinated, and di-ubiquitinated UPS reporter proteins accumulated in DA signaling mutants rather than larger poly-ubiquitinated reporter protein, which is more consistent with poly-ubiquitination impairment than it is proteasome impairment, and (ii) additional UPS reporter stabilization could be observed in DA signaling mutants when the proteasome was impaired by RNAi knockdown, which indicates that the proteasome is still removing any poly-ubiquitinated reporter protein that does form in these mutants. Our working model is that particularly unstable proteins like the UPS reporter can no longer be as efficiently poly-ubiquitinated and removed because the poly-ubiquitination machinery is otherwise occupied by trying to offset global proteome damage (Fig 5). Consistent with this model, we found that mutants with an impaired xenobiotic response are more sensitive to proteotoxic stress. Moreover, DA signaling mutants show an upregulation of proteins involved in unfolded protein stress response (e.g., heat-shock protein expression) and proteins involved in the UPS (e.g., *cul-6* and multiple F-box E3 ligases), suggesting that in the absence of DA signaling, epithelial cells are upregulating proteostasis mechanisms to compensate for the increased burden of damaged and misfolded proteins. In wild-type animals, dopamine signaling and the resulting xenobiotic response would minimize the accumulation of damaged proteins to a low enough level that the various proteostasis mechanisms (i.e., the poly-ubiquitination machinery, the proteasome, aggregation of ubiquitinated insoluble proteins into inclusion bodies, and autophagy) can handle them. It remains a formal possibility that the detoxification pathway is also required to remove one or more xenobiotic compounds that would otherwise impair the poly-ubiquitination machinery directly, although this seems less likely given the diverse set of toxins (e.g., paraquat, heat shock, cadmium ions, ethanol) that can impair UPS reporter turnover (Segref *et al*, 2011). Regardless of the specific mechanism, the resulting maintenance of proteostasis, along with the expression of other innate immunity factors, helps barrier epithelia repel infection. This signaling system might counteract that of serotonin, which is released from the chemosensory neuron ADF to negatively regulate, through a separate mechanism, innate immune response, including the rectal swelling that occurs in nematodes exposed to the pathogenic bacteria *Microbacterium nematophilum* (Anderson *et al*, 2013). Our findings demonstrate a novel example of how a multicellular organism can use its nervous system to sense environmental challenges and modulate proteostasis in target tissues using a known neurohormonal signal.

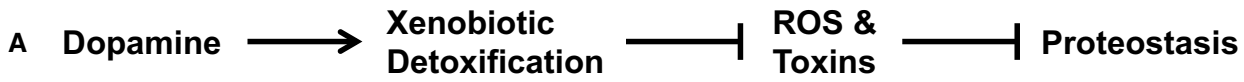

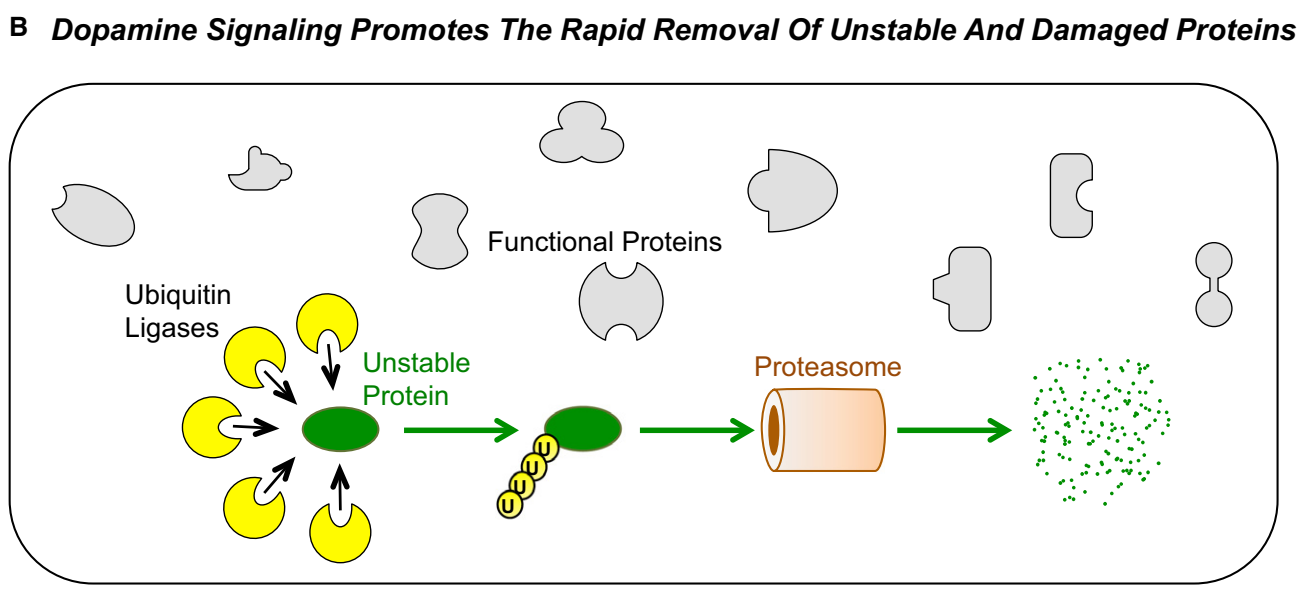

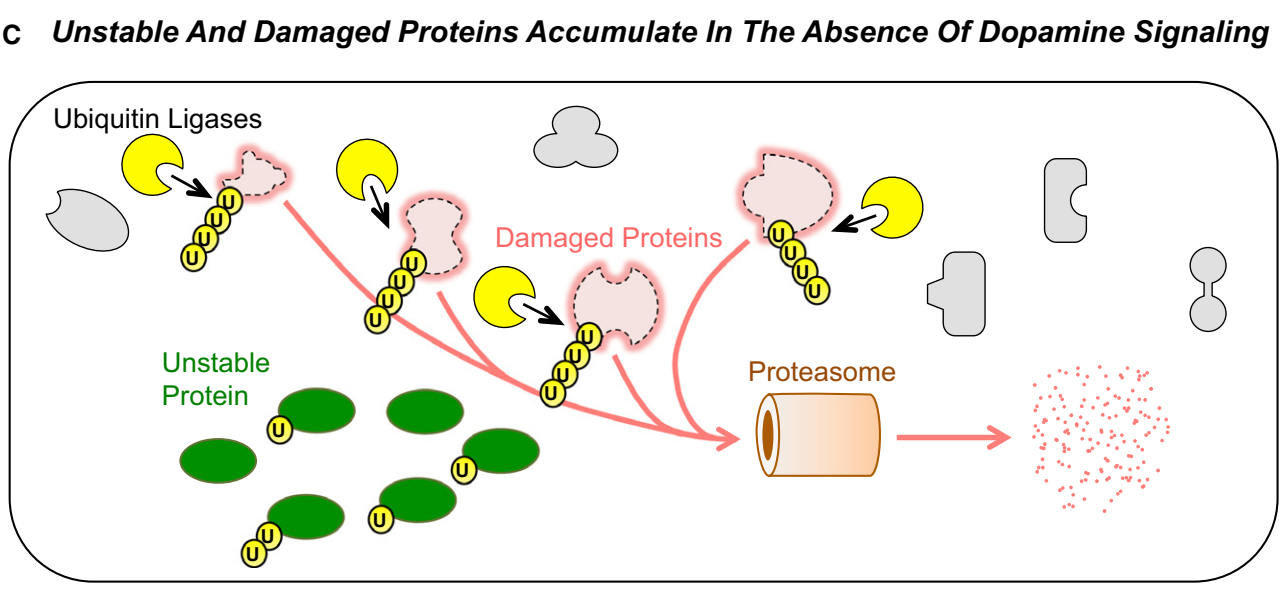

Figure 5. A hypothesized model for dopamine signaling modulation of proteostasis.

A A simple regulatory model for DA signaling and proteostasis. When nematodes encounter a bacterial lawn, the lawn's viscosity is sensed by dopaminergic mechanosensory neurons, which then release the neurohormone dopamine (DA) into the pseudocoelomic body cavity in response. DA signaling activates the expression of xenobiotic detoxification genes in epithelial tissues. The products of these genes remove toxins and ROS, which otherwise would damage proteins. Arrows indicate positive relationships, whereas T bars indicate inhibitory relationships.

B DA signaling, through activation of the xenobiotic response, protects most proteins (gray shapes) from proteotoxic stress due to toxins and ROS. Protein quality control mechanisms like the UPS (particularly, E3 and E4 ubiquitin ligases, indicated by yellow circles) are fully available to act on unstable proteins (green oval), thereby triggering the rapid ubiquitination and degradation of such proteins. Individual ubiquitin molecules are indicated by small circles with the letter "U".

C In the absence of DA signaling, there is less activation of the xenobiotic response and thus many proteins within epithelial cells become damaged by toxins and ROS (red shapes comprising dotted lines). Protein quality control mechanisms like the UPS (yellow circles) become overwhelmed ubiquitinating and degrading the large load of stressed proteins, leaving few of them available to process unstable proteins (green oval). The result is an observed stabilization of such proteins, many of which are not ubiquitinated or only partially ubiquitinated. Individual ubiquitin molecules are indicated by small circles with the letter "U".

A role for dopamine in proteostasis might transcend nematodes. In mammals, dopaminergic neurons are particularly susceptible to oxidative and metabolic stress, environmental toxins, and drugs of abuse, which in turn can increase the risk for Parkinson's disease (PD) (Ferrucci *et al*, 2008; Ares-Santos *et al*, 2013; Taylor *et al*, 2013; Friend *et al*, 2014). The resulting changes in dopaminergic signaling in PD contribute to physiological decline in neuronal and non-neuronal DA targets (Miller & O'Callaghan, 2014; Stayte & Vissel, 2014). Our findings suggest that DA regulates multiple factors that maintain proteostasis, and we speculate that loss of proteostasis due to impairments in DA signaling could be an important factor exacerbating physiological decline in PD- and DA-associated drug abuse.

Materials and Methods

Strains and growth conditions

Standard methods were used to culture *C. elegans* (Brenner, 1974). Animals were grown at 20°C on standard NGM plates seeded with OP50 *Escherichia coli*. The following strains were provided by the *Caenorhabditis* Genetics Center and were backcrossed to the laboratory N2 wild-type strain three to six times: *cat-2(e1112), dop-1(vs100), dop-1(vs101), dop-1(ok398), dop-2(vs105), dop-3(ok295), dop-3(vs106), dop-4(tm1392), dop-4(ok1321), dop-5(ok568), mec-5(ok3313), trp-4 (sy695), daf-16(mgDf50), crh-2(gk3293), skn-1(tm3411)*. Transgenic strains *odIs77[P_{col-19}::Ub^{G76V}-GFP, P_{col-19}::mRFP], norSci1[P_{dat-1}::trp-4 (d), unc-119(+)]; unc-119(ed3); vtIs1[P_{dat-1}::gfp, rol-6dm]* (a gift from M. Doitsidou, University of Edinburgh), *dgEx80[P_{vha-6}::PolyQ44::YFP, rol-6dm], vsIs28[P_{dop-1}::GFP], adEx1647[P_{dop-1}::GFP]*, and *hhIs64[P_{sur-5}::Ub^{G76V}-GFP, unc-119(+)]III; hhIs73[P_{sur-5}::mCherry, unc-119(+)]* (a gift from T. Hoppe, University of Cologne) have been described previously (Tsalik *et al*, 2003; Chase *et al*, 2004; Mohri-Shiomi & Garsin, 2008; Liu *et al*, 2011; Segref *et al*, 2011). When possible, researchers were blinded to the genotype of the observed sample.

Statistics

Twenty animals were chosen per genotype so as to observe an effect size at least as large as the coefficient of variation. All data with normal distributions were analyzed with GraphPad Prism 6 in most cases using ANOVA with Dunnett's *post hoc* test or a Student's *t*-test (two-tailed) with Holm–Sidak correction for multiple comparisons.

RNA-seq analysis

Developmentally synchronized animals were obtained by hypochlorite treatment of gravid adults to release embryos. Synchronized embryos were hatched on NGM plates and grown at 20°C until 48 h after the L4 stage of development. Fluorodeoxyuridine was used to prevent the development of second-generation embryos once animals reached fertile adulthood (Gandhi *et al*, 1980). For each RNA-seq experiment, populations for *odIs77[P_{col-19}::Ub^{G76V}-GFP]* and *dop-1(vs100); [P_{col-19}::Ub^{G76V}-GFP]* were grown simultaneously under the same conditions. Total RNA was isolated from animals using TRIzol (Invitrogen) combined with bead beater lysis in 3 biological replicates, and an mRNA library (single-end, 50-bp reads) was prepared for each sample/replicate using Illumina Truseq with PolyA selection (RUCDR). Libraries were sequenced on an Illumina HiSeq 2500 in Rapid Run Mode, resulting in high-quality sequence reads (FAST QC Phred score average of 40 out of the full 50 bp length). Reads (45–49 million per genome and replicate) were analyzed using Geospiza Genesifter, with alignment to the *C. elegans* genome (WS220) via Illumina WTS BWA (GATKv3). From 89–90% of reads mapped to the genome (72–74% mapped to annotated ORFs). Normalization and statistical analysis was performed with EdgeR with a Benjamini and Hochberg correction. Lists of differentially expressed genes were analyzed by DAVID (v6.7, david.abcc.ncifcrf.gov/home.jsp) using functional annotation clustering and a low classification stringency as the method for assessing annotation enrichment. RNA-seq datasets are available in NIH/NCBI GEO through accession number GSE80807.

RNAi feeding

RNAi feeding protocols were as described previously (Timmons *et al*, 2001). The RNAi screen was performed with 2,072 clones from the Ahringer RNAi library (Kamath *et al*, 2003; Sieburth *et al*, 2005) in animals with the *odIs77* transgene in an otherwise wild-type genetic background. *E. coli* (HT115) producing dsRNA for individual genes was seeded onto NGM plates containing 25 μg/ml carbenicillin and 0.2% lactose to induce the expression of the dsRNA for the gene of interest. The negative control was conducted by seeding the plates with HT115 containing empty vector pL4440. Synchronized embryos were hatched on each plate and grown at 20°C until 48 h after the L4 stage of development. Each clone in the screen was assessed in two independent RNAi experiments. Positives for one or both experiments were assessed a third time, and any clone that gave a positive phenotype for two or three of the experiments was included in the collection of 31 positives from the screen. It should be noted that UGT genes, CYP genes, and proteasome subunit genes were not included in the screened library. To assess knockdown phenotypes for these genes, we performed directed experiments with feeding RNAi bacteria using the procedure above. The respective clones contained sequences for *ugt-3, ugt-8, ugt-11, ugt-13, ugt-37, ugt-57, ugt-62, ugt-63, ugt-64, cyp-25A1, cyp-34A4, cyp-34A7, cyp-34A8, cyp-29A2, rpn-11, pbs-4, pbs-5, ufd-1, hsp-4, hsp-16.2, hsp-16.11, hsp-16.41, hsp-16.48, hsp-16.49, hsp-17*, and *hsp-43* in RNAi vectors; these were obtained from Open Biosystems.

Fluorescence microscopy, imaging analysis, and intensity measurements

GFP-, mRFP-, and mCherry-tagged fluorescent proteins were visualized in nematodes by mounting on 2% agarose pads with 10 mM tetramisole. Fluorescent images were observed using an Axioplan II (Carl Zeiss, Thornwood, NY). A 5× (numerical aperture 0.15) PlanApo objective was used to detect GFP and mRFP signal. Imaging was done with an ORCA charge-coupled device camera (Hamamatsu, Bridgewater, NJ) by using iVision software (Biovision Technologies, Uwchlan, PA). Exposure times were chosen to capture at least 95% of the dynamic range of fluorescent intensity of all samples. GFP fluorescence was quantified by obtaining outlines of worms using images of the mRFP or mCherry control in case of

hypodermis and intestine, respectively. The mean fluorescence intensity within each outline was calculated (after subtracting away background coverslip fluorescence) for Ub^{G76V}-GFP, mRFP and mCherry signals.

Measurement of 26S proteasome activity, GFP levels, and RFP levels in lysates

Developmentally synchronized 48-h staged animals were lysed in lysis buffer (50 mM HEPES, pH 7.5, 150 mM NaCl, 5 mM EDTA, 2 mM ATP, 1 mM dithiothreitol and protease inhibitor cocktail tablets; Roche) using a Mini Bead Beater 16 (Biospec). Lysates were transferred to microcentrifuge tubes and centrifuged at 18,000 *g* for 15 min at 4°C.

To measure proteasome activity, an equal amount of protein lysate (5 μg in 20 μl lysis buffer) was premixed with either 250 ng of proteasome inhibitor (epoxomicin, Boston Biochem, prepared in 50% dimethyl sulfoxide) or an equivalent volume of vehicle (50% dimethyl sulfoxide lacking the inhibitor), followed by the addition of proteasome assay buffer (200 μl; 25 mM HEPES, pH 7.5 and 0.5 mM ethylenediaminetetraacetic acid) containing a chymotryptic substrate (80 μM Suc-Leu-Leu-Val-Tyr-AMC; Boston Biochem). Reactions were incubated at 25 °C for 1 h, and fluorescence (λex = 360 nm; λem = 465 nm) was detected after every 5 min using a Tecan Infinite F200 detector. Epoxomicin-sensitive activity was generated with triplicate measurements from two independent experiments, quantified, and plotted.

To measure GFP and RFP in lysates, 5 μg of lysate in 100 μl of lysis buffer was placed in a 96-well plate, in duplicate. GFP and RFP fluorescence was detected using a Tecan Infinite F200 detector using a filter set for either GFP (λex = 485 nm; λem = 535 nm) or RFP (λexe = 590 nm; λem = 635). Relative fluorescence values were calculated.

Slow-killing assays and survival analysis

Using a slow-killing (SK) assay, nematodes were challenged with an infective strain of *Pseudomonas aeruginosa* (PA14). More than 50 L4 stage nematodes were transferred from NGM-OP50 to SK plates containing the pre-grown bacterial lawn of *P. aeruginosa* and incubated at 20°C (Powell & Ausubel, 2008). SK plates were prepared with 50 μg/ml of 5-fluoro-2′-deoxyuridine (FUdR), which prevents the growth of egg offspring during the experiment. *E. coli* OP50 was fed nematodes as a negative control strain with limited killing of *C. elegans* during experimental time course. Nematodes were monitored throughout a 150-h period under a dissection microscope to detect unresponsive and dead worms. Survival analyses were performed using the Kaplan–Meier method, and the significance of differences between survival curves calculated using Prism (GraphPad Software). Heat-shock survival was assessed by placing nematodes of the indicated stage at 34°C for 6 h, allowing them to recover for 1 h at 20°C, and then scoring live versus dead animals based on pharyngeal pumping and locomotion.

Western blotting and antibodies

Protein samples (30 μl) were prepared from 20 or 30 nematodes, depending upon hypodermis or intestine reporter, synchronized at L4, and lysed at 48 h post-L4 for *odIs77* and the various mutants. Equal amounts of protein samples were resolved by electrophoresis through 12% SDS–polyacrylamide gel (Bio-Rad). Western blotting was performed using mouse anti-Ub (1:2,000, Enzo), mouse anti-GFP (1:2,000, Roche), rabbit anti-PSMD14 (1:1,000, Novus), mouse anti-20S alpha 1–7 (1:1,000, Abcam), and mouse anti-actin (1:5,000, Millipore). Western blotted proteins were visualized and quantified using fluorescent-conjugated secondary antibodies from Odyssey and Licor imaging system. Each experiment was repeated at least five times with lysates from separate nematode preparations.

Expanded View for this article is available online.

Acknowledgements
We thank Gang Liu and Tejash Shah for sharing their initial studies using the UPS GFP reporter. We thank Stephanie Pyonteck for her guidance and help concerning the RNA-seq analysis. We thank M. Doitsidou, A. Fire, the *C. elegans* Genetics Center, S. Mitani, D. Garsin, T. Hoppe, S. Xu, and the Japanese National Bioresource Project for reagents and strains. We thank Kiran Madura for advice on measuring the proteasome and the use of Tecan plate reader. We thank members of the Rongo laboratory for comments on the manuscript. The manuscript was funded by grants from the National Institutes of Health (R01 NS42023 and R01 GM101972, to C.R.), as well as the New Jersey Commission on Cancer Research and the Charles and Johanna Busch Fellowship (to K.K.J.); these agencies had no other role in the research or the manuscript.

Author contributions
KKJ designed the genetic, molecular, behavioral, and cell biological experiments under the direct supervision of CR. KKJ and TLM collected the data and analyzed the results under the direct supervision of CR. CR and KKJ wrote the manuscript, with significant editorial input and discussion of their results from TLM.

Conflict of interest
The authors declare that they have no conflict of interest.

References

Aballay A (2013) Role of the nervous system in the control of proteostasis during innate immune activation: Insights from *C. elegans*. *PLoS Pathog* 9: e1003433

Akerfelt M, Morimoto RI, Sistonen L (2010) Heat shock factors: integrators of cell stress, development and lifespan. *Nat Rev Mol Cell Biol* 11: 545 – 555

An JH, Blackwell TK (2003) SKN-1 links *C. elegans* mesendodermal specification to a conserved oxidative stress response. *Genes Dev* 17: 1882 – 1893

Anders S, Huber W (2010) Differential expression analysis for sequence count data. *Genome Biol* 11: r106

Anderson A, Laurenson-Schafer H, Partridge FA, Hodgkin J, Mcmullan R (2013) Serotonergic chemosensory neurons modify the *C. elegans* immune response by regulating g-protein signaling in epithelial cells. *PLoS Pathog* 9: e1003787

Araya CL, Kawli T, Kundaje A, Jiang L, Wu B, Vafeados D, Terrell R, Weissdepp P, Gevirtzman L, Mace D, Niu W, Boyle AP, Xie D, Ma L, Murray JI, Reinke V, Waterston RH, Snyder M (2014) Regulatory analysis of the *C. elegans* genome with spatiotemporal resolution. *Nature* 512: 400 – 405

Ares-Santos S, Granado N, Moratalla R (2013) The role of dopamine receptors in the neurotoxicity of methamphetamine. *J Intern Med* 273: 437 – 453

Beaulieu JM, Gainetdinov RR (2011) The physiology, signaling, and pharmacology of dopamine receptors. *Pharmacol Rev* 63: 182 – 217

Bock KW (2014) Homeostatic control of xeno- and endobiotics in the drug-metabolizing enzyme system. *Biochem Pharmacol* 90: 1 – 6

Brenner S (1974) The genetics of *C. elegans*. *Genetics* 77: 71 – 94

Budovskaya YV, Wu K, Southworth LK, Jiang M, Tedesco P, Johnson TE, Kim SK (2008) An *elt-3/elt-5/elt-6* gata transcription circuit guides aging in *C. elegans*. *Cell* 134: 291 – 303

Butt TR, Khan MI, Marsh J, Ecker DJ, Crooke ST (1988) Ubiquitin-metallothionein fusion protein expression in yeast. a genetic approach for analysis of ubiquitin functions. *J Biol Chem* 263: 16364 – 16371

Cadet JL, Jayanthi S, Mccoy MT, Beauvais G, Cai NS (2010) Dopamine d1 receptors, regulation of gene expression in the brain, and neurodegeneration. *CNS Neurol Disord Drug Targets* 9: 526 – 538

Chang HC, Paek J, Kim DH (2011) Natural polymorphisms in *C. elegans* hecw-1 e3 ligase affect pathogen avoidance behaviour. *Nature* 480: 525 – 529

Chase DL, Pepper JS, Koelle MR (2004) Mechanism of extrasynaptic dopamine signaling in *Caenorhabditis elegans*. *Nat Neurosci* 7: 1096 – 1103

Choe KP, Leung CK, Miyamoto MM (2012) Unique structure and regulation of the nematode detoxification gene regulator, skn-1: implications to understanding and controlling drug resistance. *Drug Metab Rev* 44: 209 – 223

Ciechanover A, Kwon YT (2015) Degradation of misfolded proteins in neurodegenerative diseases: therapeutic targets and strategies. *Exp Mol Med* 47: e147

Ciechanover A, Stanhill A (2014) The complexity of recognition of ubiquitinated substrates by the 26s proteasome. *Biochim Biophys Acta* 1843: 86 – 96

Cooper DM, Bier-Laning CM, Halford MK, Ahlijanian MK, Zahniser NR (1986) Dopamine, acting through d-2 receptors, inhibits rat striatal adenylate cyclase by a gtp-dependent process. *Mol Pharmacol* 29: 113 – 119

Cortes CJ, La Spada AR (2015) Autophagy in polyglutamine disease: imposing order on disorder or contributing to the chaos? *Mol Cell Neurosci* 66: 53 – 61

Da Huang W, Sherman BT, Lempicki RA (2009a) Bioinformatics enrichment tools: paths toward the comprehensive functional analysis of large gene lists. *Nucleic Acids Res* 37: 1 – 13

Da Huang W, Sherman BT, Lempicki RA (2009b) Systematic and integrative analysis of large gene lists using david bioinformatics resources. *Nat Protoc* 4: 44 – 57

Dantuma NP, Lindsten K, Glas R, Jellne M, Masucci MG (2000) Short-lived green fluorescent proteins for quantifying ubiquitin/proteasome-dependent proteolysis in living cells. *Nat Biotechnol* 18: 538 – 543

Du H, Gu G, William CM, Chalfie M (1996) Extracellular proteins needed for *C. elegans* mechanosensation. *Neuron* 16: 183 – 194

Emtage L, Gu G, Hartwieg E, Chalfie M (2004) Extracellular proteins organize the mechanosensory channel complex in *C. elegans* touch receptor neurons. *Neuron* 44: 795 – 807

Ferrucci M, Pasquali L, Paparelli A, Ruggieri S, Fornai F (2008) Pathways of methamphetamine toxicity. *Ann N Y Acad Sci* 1139: 177 – 185

Friend DM, Fricks-Gleason AN, Keefe KA (2014) Is there a role for nitric oxide in methamphetamine-induced dopamine terminal degeneration? *Neurotox Res* 25: 153 – 160

Gandhi S, Santelli J, Mitchell DH, Stiles JW, Sanadi DR (1980) A simple method for maintaining large, aging populations of *Caenorhabditis elegans*. *Mech Ageing Dev* 12: 137 – 150

Gerstein MB, Lu ZJ, Van Nostrand EL, Cheng C, Arshinoff BI, Liu T, Yip KY, Robilotto R, Rechtsteiner A, Ikegami K, Alves P, Chateigner A, Perry M, Morris M, Auerbach RK, Feng X, Leng J, Vielle A, Niu W, Rhrissorrakrai K *et al* (2010) Integrative analysis of the *Caenorhabditis elegans* genome by the modencode project. *Science (New York, NY)* 330: 1775 – 1787

Howard RA, Sharma P, Hajjar C, Caldwell KA, Caldwell GA, Du Breuil R, Moore R, Boyd L (2007) Ubiquitin conjugating enzymes participate in polyglutamine protein aggregation. *BMC Cell Biol* 8: 32

Hsu AL, Murphy CT, Kenyon C (2003) Regulation of aging and age-related disease by daf-16 and heat-shock factor. *Science* 300: 1142 – 1145

Inoue H, Hisamoto N, An JH, Oliveira RP, Nishida E, Blackwell TK, Matsumoto K (2005) The *C. elegans* p38 mapk pathway regulates nuclear localization of the transcription factor skn-1 in oxidative stress response. *Genes Dev* 19: 2278 – 2283

Johnson ES, Ma PC, Ota IM, Varshavsky A (1995) A proteolytic pathway that recognizes ubiquitin as a degradation signal. *J Biol Chem* 270: 17442 – 17456

Kamath RS, Fraser AG, Dong Y, Poulin G, Durbin R, Gotta M, Kanapin A, Le Bot N, Moreno S, Sohrmann M, Welchman DP, Zipperlen P, Ahringer J (2003) Systematic functional analysis of the *Caenorhabditis elegans* genome using rnai. *Nature* 421: 231 – 237

Kang L, Gao J, Schafer WR, Xie Z, Xu XZ (2010) *C. elegans* trp family protein *trp-4* is a pore-forming subunit of a native mechanotransduction channel. *Neuron* 67: 381 – 391

Kebabian JW, Petzold GL, Greengard P (1972) Dopamine-sensitive adenylate cyclase in caudate nucleus of rat brain, and its similarity to the "dopamine receptor". *Proc Natl Acad Sci USA* 69: 2145 – 2149

Kindt KS, Quast KB, Giles AC, De S, Hendrey D, Nicastro I, Rankin CH, Schafer WR (2007) Dopamine mediates context-dependent modulation of sensory plasticity in *C. elegans*. *Neuron* 55: 662 – 676

Kirkin V, Mcewan DG, Novak I, Dikic I (2009) A role for ubiquitin in selective autophagy. *Mol Cell* 34: 259 – 269

Li W, Feng Z, Sternberg PW, Xu XZ (2006) A *C. elegans* stretch receptor neuron revealed by a mechanosensitive trp channel homologue. *Nature* 440: 684 – 687

Lim J, Yue Z (2015) Neuronal aggregates: formation, clearance, and spreading. *Dev Cell* 32: 491 – 501

Lindblom TH, Dodd AK (2006) Xenobiotic detoxification in the nematode *Caenorhabditis elegans*. *J Exp Zool A Comp Exp Biol* 305: 720 – 730

Lindsten K, Menendez-Benito V, Masucci MG, Dantuma NP (2003) A transgenic mouse model of the ubiquitin/proteasome system. *Nat Biotechnol* 21: 897 – 902

Lints R, Emmons SW (1999) Patterning of dopaminergic neurotransmitter identity among *Caenorhabditis elegans* ray sensory neurons by a tgfbeta family signaling pathway and a hox gene. *Development* 126: 5819 – 5831

Liu G, Rogers J, Murphy CT, Rongo C (2011) EGF signalling activates the ubiquitin proteasome system to modulate *C. elegans* lifespan. *EMBO J* 30: 2990 – 3003

Mair W, Morantte I, Rodrigues AP, Manning G, Montminy M, Shaw RJ, Dillin A (2011) Lifespan extension induced by AMPK and calcineurin is mediated by *crtc-1* and CREB. *Nature* 470: 404 – 408

Mardones P, Martinez G, Hetz C (2015) Control of systemic proteostasis by the nervous system. *Trends Cell Biol* 25: 1 – 10

Meisel JD, Panda O, Mahanti P, Schroeder FC, Kim DH (2014) Chemosensation of bacterial secondary metabolites modulates neuroendocrine signaling and behavior of *C. elegans*. *Cell* 159: 267 – 280

Miller DB, O'Callaghan JP (2014) Biomarkers of Parkinson's Disease (PD): present and future. *Metabolism* 64: S40 – S46

Miyabayashi T, Palfreyman MT, Sluder AE, Slack F, Sengupta P (1999) Expression and function of members of a divergent nuclear receptor family in *Caenorhabditis elegans*. *Dev Biol* 215: 314 – 331

Mohri-Shiomi A, Garsin DA (2008) Insulin signaling and the heat shock response modulate protein homeostasis in the *Caenorhabditis elegans* intestine during infection. *J Biol Chem* 283: 194 – 201

Morley JF, Brignull HR, Weyers JJ, Morimoto RI (2002) The threshold for polyglutamine-expansion protein aggregation and cellular toxicity is dynamic and influenced by aging in *Caenorhabditis elegans*. *Proc Natl Acad Sci USA* 99: 10417 – 10422

Murphy CT, Mccarroll SA, Bargmann CI, Fraser A, Kamath RS, Ahringer J, Li H, Kenyon C (2003) Genes that act downstream of *daf-16* to influence the lifespan of *Caenorhabditis elegans*. *Nature* 424: 277 – 283

Murshid A, Eguchi T, Calderwood SK (2013) Stress proteins in aging and life span. *Int J Hyperthermia* 29: 442 – 447

Nagarajan A, Ning Y, Reisner K, Buraei Z, Larsen JP, Hobert O, Doitsidou M (2014) Progressive degeneration of dopaminergic neurons through trp channel-induced cell death. *J Neurosci* 34: 5738 – 5746

Nguyen T, Nioi P, Pickett CB (2009) The Nrf2-antioxidant response element signaling pathway and its activation by oxidative stress. *J Biol Chem* 284: 13291 – 13295

Oliveira RP, Porter Abate J, Dilks K, Landis J, Ashraf J, Murphy CT, Blackwell TK (2009) Condition-adapted stress and longevity gene regulation by *Caenorhabditis elegans* SKN-1/Nrf. *Aging Cell* 8: 524 – 541

Papp D, Csermely P, Soti C (2012) A role for SKN-1/Nrf in pathogen resistance and immunosenescence in *Caenorhabditis elegans*. *PLoS Pathog* 8: e1002673

Park SK, Tedesco PM, Johnson TE (2009) Oxidative stress and longevity in *Caenorhabditis elegans* as mediated by *skn-1*. *Aging Cell* 8: 258 – 269

Pellegrino MW, Nargund AM, Kirienko NV, Gillis R, Fiorese CJ, Haynes CM (2014) Mitochondrial UPR-regulated innate immunity provides resistance to pathogen infection. *Nature* 516: 414 – 417

Powell JR, Ausubel FM (2008) Models of *Caenorhabditis elegans* infection by bacterial and fungal pathogens. *Methods Mol Biol* 415: 403 – 427

Prahlad V, Cornelius T, Morimoto RI (2008) Regulation of the cellular heat shock response in *Caenorhabditis elegans* by thermosensory neurons. *Science* 320: 811 – 814

Pukkila-Worley R, Feinbaum RL, Mcewan DL, Conery AL, Ausubel FM (2014) The evolutionarily conserved mediator subunit *mdt-15*/med15 links protective innate immune responses and xenobiotic detoxification. *PLoS Pathog* 10: e1004143

Runkel ED, Liu S, Baumeister R, Schulze E (2013) Surveillance-activated defenses block the ros-induced mitochondrial unfolded protein response. *PLoS Genet* 9: e1003346

Ryno LM, Wiseman RL, Kelly JW (2013) Targeting unfolded protein response signaling pathways to ameliorate protein misfolding diseases. *Curr Opin Chem Biol* 17: 346 – 352

Sanyal S, Wintle RF, Kindt KS, Nuttley WM, Arvan R, Fitzmaurice P, Bigras E, Merz DC, Hebert TE, Van Der Kooy D, Schafer WR, Culotti JG, Van Tol HH (2004) Dopamine modulates the plasticity of mechanosensory responses in *Caenorhabditis elegans*. *EMBO J* 23: 473 – 482

Saul N, Pietsch K, Menzel R, Steinberg CE (2008) Quercetin-mediated longevity in *Caenorhabditis elegans*: is *daf-16* involved? *Mech Ageing Dev* 129: 611 – 613

Sawin ER, Ranganathan R, Horvitz HR (2000) *C. elegans* locomotory rate is modulated by the environment through a dopaminergic pathway and by experience through a serotonergic pathway. *Neuron* 26: 619 – 631

Segref A, Torres S, Hoppe T (2011) A screenable in vivo assay to study proteostasis networks in *Caenorhabditis elegans*. *Genetics* 187: 1235 – 1240

Shore DE, Ruvkun G (2013) A cytoprotective perspective on longevity regulation. *Trends Cell Biol* 23: 409 – 420

Sieburth D, Ch'ng Q, Dybbs M, Tavazoie M, Kennedy S, Wang D, Dupuy D, Rual JF, Hill DE, Vidal M, Ruvkun G, Kaplan JM (2005) Systematic analysis of genes required for synapse structure and function. *Nature* 436: 510 – 517

Stayte S, Vissel B (2014) Advances in non-dopaminergic treatments for Parkinson 's disease. *Front Neurosci* 8: 113

Sun J, Liu Y, Aballay A (2012) Organismal regulation of *xbp-1*-mediated unfolded protein response during development and immune activation. *EMBO Rep* 13: 855 – 860

Sun J, Singh V, Kajino-Sakamoto R, Aballay A (2011) Neuronal GPCR controls innate immunity by regulating noncanonical unfolded protein response genes. *Science* 332: 729 – 732

Suo S, Ishiura S (2013) Dopamine modulates acetylcholine release via octopamine and creb signaling in *Caenorhabditis elegans*. *PLoS ONE* 8: e72578

Tatum MC, Ooi FK, Chikka MR, Chauve L, Martinez-Velazquez LA, Steinbusch HW, Morimoto RI, Prahlad V (2015) Neuronal serotonin release triggers the heat shock response in *C. elegans* in the absence of temperature increase. *Curr Biol* 25: 163 – 174

Taylor JM, Main BS, Crack PJ (2013) Neuroinflammation and oxidative stress: co-conspirators in the pathology of parkinson's disease. *Neurochem Int* 62: 803 – 819

Tepper RG, Ashraf J, Kaletsky R, Kleemann G, Murphy CT, Bussemaker HJ (2013) PQM-1 complements *daf-16* as a key transcriptional regulator of *daf-2*-mediated development and longevity. *Cell* 154: 676 – 690

Timmons L, Court DL, Fire A (2001) Ingestion of bacterially expressed dsrnas can produce specific and potent genetic interference in *Caenorhabditis elegans*. *Gene* 263: 103 – 112

Treweek TM, Meehan S, Ecroyd H, Carver JA (2015) Small heat-shock proteins: important players in regulating cellular proteostasis. *Cell Mol Life Sci* 72: 429 – 451

Tsalik EI, Niacaris T, Wenick AS, Pau K, Avery L, Hobert O (2003) LIM homeobox gene-dependent expression of biogenic amine receptors in restricted regions of the *C. elegans* nervous system. *Dev Biol* 263: 81 – 102

Van Oosten-Hawle P, Porter RS, Morimoto RI (2013) Regulation of organismal proteostasis by transcellular chaperone signaling. *Cell* 153: 1366 – 1378

Van Oosten-Hawle P, Morimoto RI (2014) Organismal proteostasis: role of cell-nonautonomous regulation and transcellular chaperone signaling. *Genes Dev* 28: 1533 – 1543

Vilchez D, Morantte I, Liu Z, Douglas PM, Merkwirth C, Rodrigues AP, Manning G, Dillin A (2012) RPN-6 determines *C. elegans* longevity under proteotoxic stress conditions. *Nature* 489: 263 – 268

Vilchez D, Saez I, Dillin A (2014) The role of protein clearance mechanisms in organismal ageing and age-related diseases. *Nat Commun* 5: 5659

Volovik Y, Moll L, Marques FC, Maman M, Bejerano-Sagie M, Cohen E (2014) Differential regulation of the heat shock factor 1 and *daf-16* by neuronal *nhl-1* in the nematode *C. elegans*. *Cell Rep* 9: 2192 – 2205

Warnatsch A, Bergann T, Kruger E (2013) Oxidation matters: the ubiquitin proteasome system connects innate immune mechanisms with MHC class I antigen presentation. *Mol Immunol* 55: 106 – 109